

# University of Groningen

## Internship Report

---

### Using Corticomuscular Coherence to Assess Cortical Contribution to Walking Gait in Patients with Parkinson's Disease

---

*Author:*  
Alok Ranjan  
(s3816494)  
M.Sc., Biomedical Engineering  
University of Groningen  
August 2019

*Internship Supervisor:*  
prof. dr. ir. Natasha M.Maurits  
Neurology Department  
University Medical Center Groningen

*Internship Second Supervisor:*  
Ms. Joyce B. Weersink  
Neurology Department  
University Medical Center Groningen

*University Supervisor:*  
prof. dr. ir. G.J. (Bart) Verkerke  
Rehabilitation-General Department  
University Medical Center Groningen

## **1. Introduction**

In quadrupeds, locomotion is achieved by the activity in the hip extensors during most of the stance phase that provides significant forward propulsion (Shapiro et al., 1994; Trank et al., 1996). The basic rhythmicity of quadrupedal locomotion is generated by spinal networks, which may function relatively independently of supraspinal control (Kiehn, 2016). In human bipedal locomotion, forward propulsion is generated by moving the center of gravity slightly in front of the supporting leg with little activity in plantar flexor muscle during the stance and push off. This difference in kinematics indicates that human gait must have required significant re-organization of the central networks involved in the generation of human gait since it first evolved (Jensen et al., 2019).

Human bipedal movement is an outcome of brain-controlled muscle activities. Like in quadrupeds, it demonstrates a characteristic of a four-limb movement pattern where the hands are in anti-phase coordination with the legs. These gait cycles are driven by rhythm generating networks in the spinal cord and brainstem, which are, however, integrated with more widespread networks that also include cortical regions (Weersink et al., 2019).

Electroencephalography (EEG) and electromyography (EMG) have been used to quantify these brain and muscle activities during gait in different studies (Halliday et al., 2003; Petersen et al., 2012; Artoni et al., 2017). These powerful techniques measure electrical activity in the brain and muscles, respectively. Analysing these measurements helps the understanding of brain and motor mechanisms and their relationships. These analyses also help in identifying nerve and muscle disorders. Movement disorders are one of the prime examples of it, that can be characterized by abnormal voluntary movements, involuntary movements, slow movement, and/or reduced movements. One prime example of a movement disorder is Parkinson's Disease (PD) that affects both motor and cognitive function (Suwansawang, 2018). Understanding human movement or the relationship between brain and muscle activity can assist to recognize the first phases of these movement disorders.

Bloomfield (1976) and Halliday et al., (1995) have explained a methodology to understand human movement with the help of spectral analysis of the obtained EEG and EMG signals. It finds out their rhythmic behaviour and dependencies between them that is further used in studies by Amjad et al., (1997) and Halliday et al., (2003) to investigate physiological tremors. A classical and popular method is to obtain the spectral representation using the

Fourier transform of these signals and using that to find out coherence, phase, and cumulant density.

PD is caused by progressive degeneration of dopaminergic cells in the substantia nigra pars compacta (SNc), resulting in striatum depletion of dopamine. The SNc's dopaminergic projections modulate the direct and indirect pathway activity by exciting the direct pathway through one type of dopamine receptor (D1) and inhibiting the indirect pathway through another type of dopamine receptor (D2). Also, inhibition action is decreased along the direct pathway from the striatum to the globus pallidus (GPi)/SNr. The inhibitory output from the GPi is increased. Thus, too much inhibitory input to the thalamus leads to a reduction in cortical activity. If about 90% of dopamine is reduced, symptoms of Parkinson, i.e. tremor, rigidity, bradykinesia, and akinesia, will become obvious (Gazzaniga et al. 2002; Suwansawang, 2018).

At the cortical level, the primary motor cortex (M1) and Supplementary Motor Area (SMA) have their importance in the gait cycle. M1 provides region-specific motor contributions that are located somatotopically in the human precentral gyrus. In contrast, the SMA has widespread and stronger connections to the contralateral cortex in comparison to M1, supporting the idea that the SMA participates in a more bilateral motor system and provides opposite limb coordination (Rouiller et al., 1994, Ruddy et al., 2017). The SMA also contributes to walking gait and its impairment can result in imbalance and abnormalities in gait. In PD, decreased activation in the SMA has been related to reduced step length and loss of arm swing in patients. Apart from its role in opposite limb coordination, SMA is associated with a wider ambit of the cortical circuitry. It also plays a pivotal role in voluntary movement initiation. Bilateral movement coordination and movement initiation together seem to provide a cyclic pattern of four limbs during gait, in which arm swing might serve as a driving force in walking. Since the SMA has immediate links to both the spinal cord and M1, its suggested function in gait monitoring can be achieved either through direct input to lower motor centers, input mediated by M1, or both (Weersink et al., 2019).

To find out the contribution of M1 and SMA activity to gait, an experiment was designed in which a group of Parkinson's patients and a group of healthy age-matched controls first walk normally and later walk with enhanced arm swing. EEG and EMG were recorded from the brain and different leg and arm muscles to further analyze the relationship between brain and muscle activity in the spectral and time domain as suggested in Halliday et al., (1995) using

NeuroSpec, an archive of MATLAB routines for multivariate Fourier analysis of time series and/or point process data (<http://www.neurospect.org/>). The analysis will try to answer the following questions:

1. Is M1 involved in leg muscle activation during gait?
2. Is the SMA, directly or indirectly through M1, involved in the activation of leg muscles during gait?
3. Are SMA and M1 involved in activation of arm muscles during gait related arm swing?

## **2. Methods**

### **2.1 Participants and Ethics Approval**

Twenty participants with Parkinson's disease (13 males and 7 females, median age 67.5 years and interquartile range 11.25 years) and twenty healthy (control) participants (10 males and 10 females, median age 69 years and interquartile range 4.25 years) participated. All participants were able to walk independently. Some of them used medication about which the information is provided in the appendix in Table 2. They underwent a mini-mental state exam (median score 29 and interquartile range 2, with no individual score less than 24) to test for their cognitive function. They were all right-handed according to the Annett Handedness scale defined in Annet, (1970). To perform the study, written consent was obtained from all participants before the start of the study. The study was executed per the Declaration of Helsinki (2013) and was approved by the ethical committee of the University Medical Center Groningen.

### **2.2 Task and Experimental Setup**

The experiment was conducted in two sessions, which were on the same day and approximately 10 minutes apart. Participants were instructed to walk at their comfortable speed through a hallway of 150 m in a straight line from start to finish and back. Turning was not included in the analysis. The first session was walking normally as a walk in the park, with a normal arm swing (anti-phase). In the second session, participants were asked to walk with an enhanced arm swing. Afterward, with the help of recorded video, it was checked whether walking with enhanced arm swing was performed correctly or not. As per the inspection, eighteen participants from the control group (C) and nineteen participants from the PD group were included for analysis of the dataset of walking with enhanced arm swing. During both sessions, monopolar EEG was recorded using a cap with 32 active Ag-AgCl electrodes (EasyCap GmbH, Herrsching, Germany) which are located on the cap according to the 10-20 system. The ground and reference electrodes were located between Fz and FCz and between Fz and Cz, respectively. The electrodes used were active, meaning that the amplification first takes place at the electrodes and therefore the artifacts because of the cable movements were considerably suppressed. 'Heel Strike' and 'Toe-Off' were also recorded for both legs during walking using a tri-axial accelerometer (Compumedics Neuroscan, Singen, Germany). The EEG and accelerometer signals were recorded and synchronized at a

sampling rate of 512 Hz and stored on a laptop for later analysis. The equipment and setup used are the same as in Weersink et al., (2019). To minimize artifacts, participants were asked to minimize eye blinks, relax the jaw muscles and to minimize swallowing during the experiment.

For the study, surface EMG from tibialis anterior (TA) at two locations, a few centimetres apart, soleus (S), rectus femoris (RF), biceps femoris (BF), deltoid anterior (DA) and deltoid posterior (DP) muscles of left and right side of the body were obtained using total 14 bipolar EMG electrodes. After careful palpation of the muscle, the skin was shaved, cleaned and electrodes were placed on the middle part of the muscle belly.

The activation in the leg muscles concerning the gait is shown in the picture below. Here, black muscle areas represent high activation, white muscle areas represent no activation and gray muscle areas represent Intermediate activation as discussed in Vaughan et al. (1999).

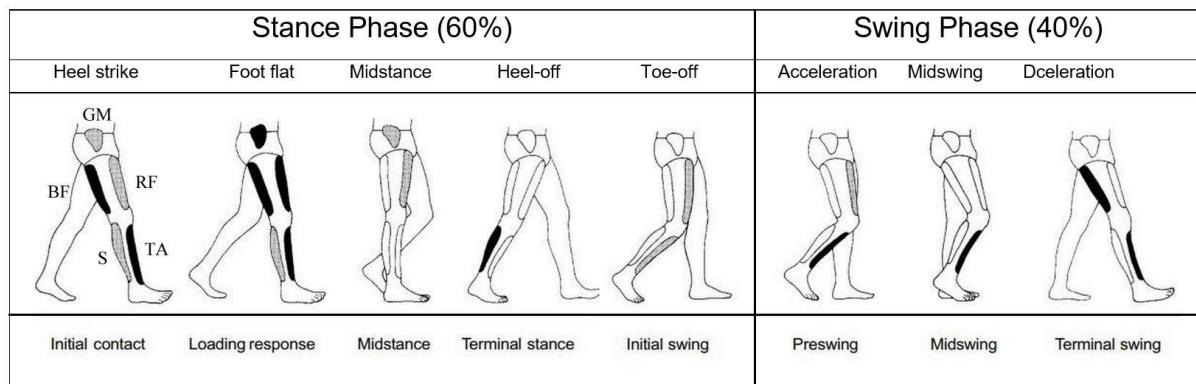


Figure 1: Phases of the gait cycle, showing the activity of the five major muscles in the lower extremity. Courtesy of Vaughan et al., (1999)

## 2.3 Gait Analysis

The exact time-points of Heel Strike and Toe-Off were determined by an approach used in Sejdic et al., (2016). It is a three-stage approach in which acceleration and deacceleration data from the accelerometer in X, Y and Z axes are used to identify the heel strike and toe-off timing. The identification for these values was performed by Ms. Weersink. The identification process for the current data set is same as in Weersink et al., (2019).

## 2.4 Data Pre-Processing

EEG data pre-processing was performed in MATLAB 2014a (The MathWorks) using EEGLAB 13\_1\_1\_b ([sccn.ucsd.edu/eeglab](http://sccn.ucsd.edu/eeglab)). EEGLAB is an open-source environment for processing electrophysiological data. The EEG data were recorded at a rate of 512Hz, but to speed up the computation and to synchronize them with EMG data, the EEG data were downsampled at a sampling rate of 256Hz. The data were high pass filtered through a finite impulse response (FIR) filter at 1 Hz with zero phase shift. Also, for removing line noise a notch filter at 50 and 100 Hz was used as per the Cleanline technique ([nitrc.org/projects/cleanline](http://nitrc.org/projects/cleanline)). Further, as a post-processing step, motion artifact cleaning was done using the technique described in Weersink et al., (2019).

The EMG data were recorded at a rate of 512Hz and later were downsampled at a frequency of 256 Hz. Further, were processed through a high pass filter of 5 Hz to remove the low-frequency noise in MATLAB 2018a. Using the ‘highpass’ function of MATLAB also compensates for the delay which is generally introduced when using moving average filters. The EMG data were not processed through a low pass filter.

## 2.5 A Framework for Analysis

NeuroSpec (<http://www.neurospect.org/>) was used for the analysis of EEG and EMG point process data. The approaches adopted in the routines are based on the finite Fourier transform. Brillinger (1993) points out that the spectra have both theoretical and physical existences and thus, the analysis can be approached from two very different viewpoints. On one hand it can be used to gain insight and inference from the data but on the other hand, it can also be used in theoretical studies. The analysis uses estimates of both time domain and frequency domain parameters and stresses the complementary nature of time and frequency domain parameters which can be used to characterize different aspects of the same data (Halliday et al., 1995). The fact that all linear time-domain parameters are estimated via the frequency domain does not, in general, affect the interpretation of these parameters. Also, some time domain and frequency domain parameters are mathematically equivalent but convey a different representation and that is why it is important to use both representations to obtain the maximum insight into and inference about the behavior of complex systems (Rosenberg et al., 1989).

If  $x$  is a rectified EMG signal and  $y$  is an EEG signal, their power spectra can be estimated by using the periodogram approach, where the discrete Fourier transforms are constructed from sections of data taken at a fixed offset time with respect to a trigger point in each cycle. Estimates of the spectra are constructed by averaging periodograms across all cycles (Petersen et al., 2012). The auto spectrum of  $x$  and  $y$  at each frequency can be estimated as  $f_{xx}(\lambda)$  and  $f_{yy}(\lambda)$ , respectively, and the cross-spectrum between  $x$  and  $y$  can be estimated as  $f_{xy}(\lambda)$  as defined in Halliday et al., (1995). The linear dependence between  $x$  and  $y$  can be defined by coherency, which is defined as the normalized cross-spectrum:

$$R_{xy}(\lambda) = \frac{f_{xy}(\lambda)}{\sqrt{f_{xx}(\lambda)f_{yy}(\lambda)}} \quad (1)$$

Its squared modulus is called coherence, which provides estimates of the strength between two processes  $x$  and  $y$ :

$$|R_{xy}(\lambda)|^2 = \frac{|f_{xy}(\lambda)|^2}{f_{xx}(\lambda)f_{yy}(\lambda)} \quad (2)$$

The timing information about the correlation can be attained from the phase spectrum,  $\phi_{xy}(\lambda)$ . As the cross-spectrum is a complex quantity, its phase can be given by its argument that can be obtained from the ‘arctan’ function. The function ‘arctan’ is generally defined over the range  $[-\pi/2, \pi/2]$ , however, the signs of the real and imaginary parts of  $f_{xy}(\lambda)$  can be used to modify the determined phase and convert it to extend the range further to  $[-\pi, \pi]$  (Halliday et al., 1995). Function ‘atan2’ of MATLAB is based on the same methodology where phase is continuous in the range of  $[-\pi, \pi]$ .

$$\phi_{xy}(\lambda) = \arg\{f_{xy}(\lambda)\} = \arctan \left\{ \frac{\text{Im}(f_{xy}(\lambda))}{\text{Re}(f_{xy}(\lambda))} \right\} \quad (3)$$

In the time domain the linear pairwise association between two processes can be characterized by second order cumulant density functions, defined by the inverse Fourier transform of the cross-spectrum  $f_{xy}(\lambda)$  as defined in Brillinger, (1974) as:

$$q_{xy}(u) = \int_{-\pi}^{\pi} f_{xy}(\lambda) e^{i\lambda u} d\lambda \quad (4)$$

Cumulant densities provide a measure of statistical dependence between random processes. If any of the processes under consideration is independent of the other process, then the value of the cumulant is zero. Cumulant densities can assume either positive or negative values.

Cumulant densities are unbounded measures of association which in practice means that, although in the null case of independent processes the asymptotic value is zero, there is no upper limit indicating a perfect linear relationship (Halliday et al., 1995). It is a customary practice to plot spectra, coherence and cumulant densities on a  $\log_{10}$  scale.

Further, estimation of confidence limits for spectra, coherence and cumulant density is done by calculating the variance, which is discussed in Halliday et al., (1995).

## 2.6 Analysis

Time-domain and frequency-domain estimates of the correlation between EEG and EMG signals were obtained for each participant through spectral estimates, which were constructed by averaging over short segments of data (Jensen et al., 2019). The user guide of NeuroSpec Version 2.0, (<http://www.neurospec.org/>) explains three types of methods to define a segment. Type 2 analysis was used for this analysis, where an offset from the trigger point defines the start of the segment and the number of offset points which defines the segment length determine the end of the segment. Only full-length segments were considered to be part of further analysis.

Time independent ( $T_{ind}$ ) and time-dependent ( $T_d$ ) plots were made to visualize coherence and phase estimates in the frequency domain and cumulant density estimates in the time domain.  $T_{ind}$  plots were used to visualize these parameters for the defined segment and using these plots, allow to look closely into the estimates of these parameters, their variation, and significance. Though it is not definite at which instance the muscle and cortical activity can show their co-variations, providing a short window of time and looking into these co-variations in detail using  $T_{ind}$  plots is time taking. Thus,  $T_d$  plots have been used to find the estimates of parameters for a bigger part of the gait cycle.  $T_d$  plots are a representation of multiple  $T_{ind}$  plots in a single figure along a time axis, thereby providing a visualization of a part of the gait cycle of interest.

For example, the relationship between EEG of cortical region Cz and EMG of muscle Tibialis Anterior's 2nd electrode of the right leg (TA2R) was obtained in the frequency and time domains. EEG and EMG, both were sampled at 512 Hz and later downsampled to 256 Hz to increase the computation rate. Heel strike data were obtained from the accelerometer, used for defining the triggers. For the  $T_{ind}$  analysis, the start of the segment was at -550 ms in

relation to the heel strike and 128 segment points after that (i.e. -50 ms) was defined as the end of the segment. This range was chosen because it corresponds to the interval before heel strike with the largest coherence estimates and maximal EMG activity for TA (Petersen et al., 2012). 128 segment points provide a frequency resolution of 2 Hz in spectral estimates. The EEG and EMG signal segments were first detrended and EMG signals were full-wave rectified to suppress information related to action potential waveform shape (Halliday and Farmer, 2010). Coherence, phase, and cumulant density were calculated for each EEG-EMG segment pair. Averaging coherence, phase and cumulant density of all pairs provide coherence, phase and cumulant density for each participant. For cumulant density the lag was plotted from -250 ms to 250 ms.

$T_d$  analysis is more complex than  $T_{ind}$  analysis. For  $T_d$  analysis, the part of the gait cycle of interest was traced at 23 points (including start and end points) i.e. from -1100 Ms to 0 ms in relation to the heel-strike. Therefore, every point on the time scale is 50 ms apart. From each tick on time scale, the next 64 points were considered as a segment for both EEG and EMG signals. These EEG and EMG segments were detrended and EMG segments were further rectified. Coherence, phase and cumulant density for these EEG-EMG segment pairs were calculated. Each tick represents the average parameter value of that segment. This can be understood using matrix representation. 64 points segments will have a frequency resolution of 4 Hz. For a 256 Hz sample, Nyquist frequency is 128 Hz. Therefore, 24 (128/4) values can be assigned in a column and 23 values (time points) can be assigned in a row, gives a 24x23 matrix. Each column of this matrix is the average value of the respective parameter (coherence, phase, and cumulant density), calculated for the 64 point segment which started just after that time tick. This 24x23 matrix represents a part of a single gait cycle of interest. If  $G$  Gait cycles were walked by one participant, there will be  $G$  such matrices for each parameter. The average of these  $G$  matrices of the respective parameter will give the final outcome of that parameter for that participant. Thus, the final value of coherence over the gait cycle will be an average of coherences of all gait cycles. Similarly, phase and cumulant density over the gait cycle will be an average of phases and cumulant densities, respectively, of all gait cycles that participant had walked. 64 point segments were used in  $T_d$  analysis, so more precision is gained in the time domain at a cost of losing frequency resolution in the spectral domain.

The matrices are plotted as heatmaps where the colors represent the value of estimates using color bar. The 95% confidence interval is calculated for estimated values and every value

below the significance level is turned to zero to only visualize the significant co-relations in the  $T_d$  contour plots as done in Jensen et al., (2019).

There are four main analyses.

1. Control group walking normal (C\_WN)
2. Control group walking with enhanced arm swing (C\_WEA)
3. Parkinson disease group walking normal (PD\_WN)
4. Parkinson disease group walking with enhanced arm swing (PD\_WEA).

After performing the individual analysis, a pooled analysis (for  $T_{ind}$  and  $T_d$ ) was performed within all four groups. The pooled coherence in the frequency domain provides the average of the coherences of all participants of the respective groups, and similarly the pooled phase is average of phases calculated for each participant in the respective group in the frequency domain and pooled cumulant density is average of cumulant densities of each participant in the respective group in the time domain. Comparison of coherence between these groups was also calculated by applying Fisher's transform,  $\text{Tan } h^{-1}$ , to the coherences of both groups of interest and finding the difference between these transforms (Amjad et. Al., 1997). Further, the results were plotted to see the difference between control and Parkinson disease group and to find out the difference in coherence while walking with and without enhanced arm swing.

Pooled analysis estimates for all four groups were calculated for the combinations in table 1:

Table 1: cortical location and muscle combinations used for analysis of estimates of different parameters

<b>Serial Number</b>	<b>EEG data from cortical region</b>	<b>EMG data from muscle</b>	<b>Side of the body</b>	<b>Heel Strike</b>
1	Cz	RF	Right leg	Right leg
2	Cz	TA	Right leg	Right leg
3	Fz	RF	Right leg	Right leg
4	Fz	TA	Right leg	Right leg
5	Fz	DA	Left shoulder	Right leg
6	C4	DA	Left shoulder	Right leg

A full gait cycle is considered from heel strike of the right leg to next heel strike of the right leg. The point process data is not normalized between heel strikes. The gait timings are varying between 1000 ms to 1200 ms. Because of such variation, the estimate of each parameter for each participant will not be normalized. This will create a bias in individual and the pooled analysis. For interpretation of results an average value i.e. 1100 ms is considered as gait cycle duration. Also, at 50% of this duration i.e. 550 ms is the heel strike of another leg.

Also, all the participants have walked different numbers of gait cycles and all of them were taken into consideration of this analysis. To have a common ground for comparison it would have been a standardization if only the minimum of the number of the gait cycles walked by all participants were considered in the analysis.

### **3. Results**

#### **3.1 Time Independent Analysis**

TA, RF and, DA were analysed under this assignment. The maximum activation duration in gait are different for these muscles. Therefore, TA was analysed from -550 ms to -50 ms (Jensen et al., 2019), RF was analysed from -1100 ms to -600 ms (Dyer et al., 2014) and DA was analysed from -950 ms to -450 ms (Jackson et al., 1978; Kuhtz-Buschbeck et al., 2012) in relation to the heel strike. The pooled generated results are plotted and are available in the appendix section.

#### **3.2 Time Dependent Analysis**

In  $T_d$  analysis, plots of the estimate of coherence, phase, and cumulant density have been obtained for the full gait cycle (i.e. -1100 ms to 0 ms in relation to the heel strike). Segment length is 64 points which give a frequency resolution of 4 Hz. Resolution on the time scale is 50 ms. Results for each EEG and EMG combination are as follows:

### 3.2.1 EEG data from cortical region Cz vs EMG data from TA

Figure 2 illustrates pooled estimates of coherence, phase and cumulant density for C\_WN between Cz and TA of the right leg. Significant low-frequency coherence (2-13 Hz) is present at midswing (around -300 ms), before and after the right heel strike (RHS) (from -200 ms to 0 ms and at -1100 ms), before and after the left heel strike (LHS) (from -800 ms to -350 ms in relation to the RHS). Beta frequency coherence of 20 Hz is present just before the LHS (at -650 ms). Gamma frequency coherence of about 40-50 Hz is present in a large region before and after the LHS (from -800 ms to -350 ms in relation to RHS).

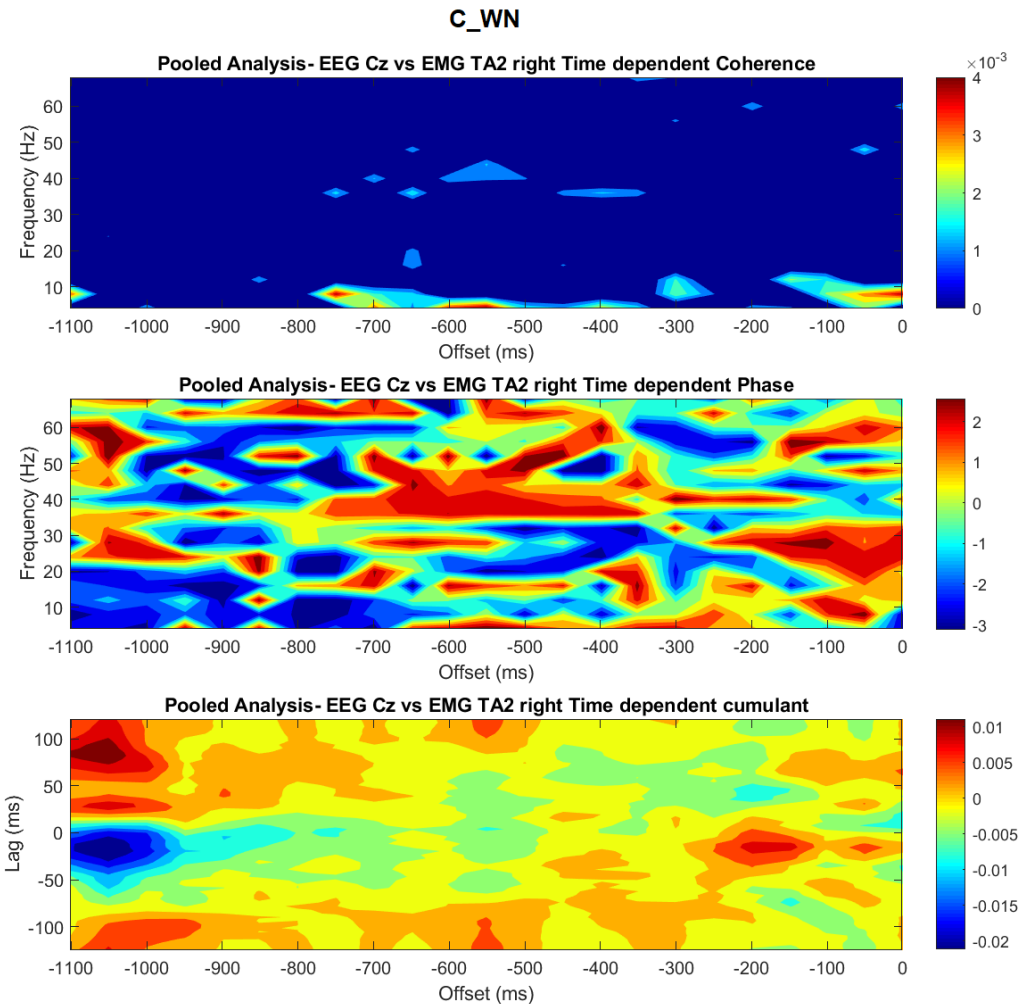


Figure 2: Shows  $T_d$  estimates of corticomuscular coupling parameters for C\_WN, i.e. coherence (top), phase (middle), cumulant density (bottom) for cortical region Cz and muscle TA of the right leg.

Figure 3 illustrates pooled estimates of coherence, phase and cumulant density for C\_WEA between Cz and TA. There is significant coherence present in low-frequency range before and after RHS (from -200 ms to 0 ms and from -1100 ms to -900 ms in relation to RHS). Also, at certain locations, significant coherence is present in the beta and gamma frequency range. Beta frequency coherence is present near LHS (at -600 ms and -500 ms of about 15 Hz), after RHS (at -1050 ms of about 24 Hz) and a strong beta coherence is present just before the RHS (from -150 ms to 0 ms of about 15 Hz). Gamma frequency coherence is present in midswing (at -200 ms of about 60 Hz) and pre-swing (at -300 ms of about 55 Hz) region.

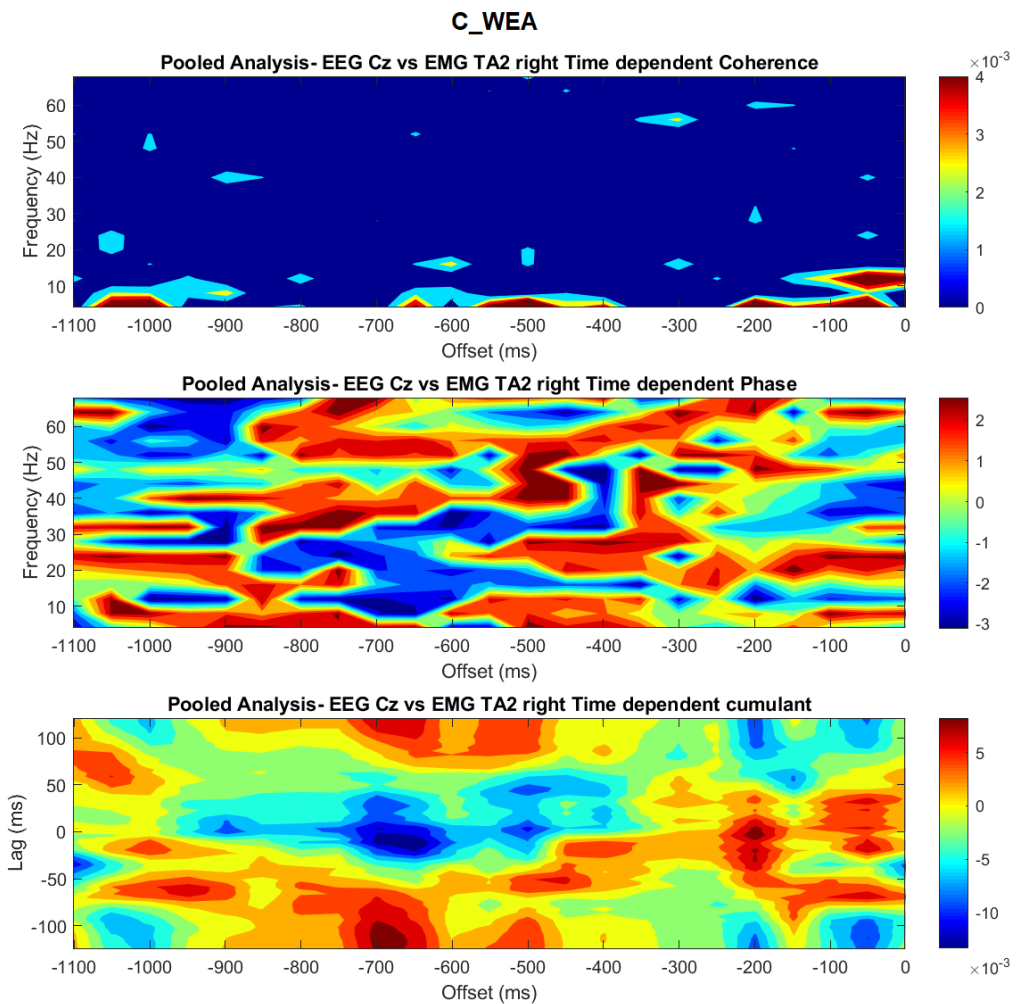


Figure 3: Shows  $T_d$  estimates of corticomuscular coupling parameters for C\_WEA, i.e. coherence (top), phase (middle), cumulant density (bottom) for cortical region Cz and muscle TA of the right leg.

Figure 4 illustrates pooled estimates of coherence, phase and cumulant density for PD\_WN between Cz and TA. Significant coherence at low frequencies for this pool is present almost over the whole gait cycle. Beta coherence is present at certain locations before and after the heel strike (from -800 ms to -200 ms, of about 20 Hz). Gamma frequency coherence of 40 Hz and 50 Hz is present in the swing phase at -400 ms and -100 ms, respectively.

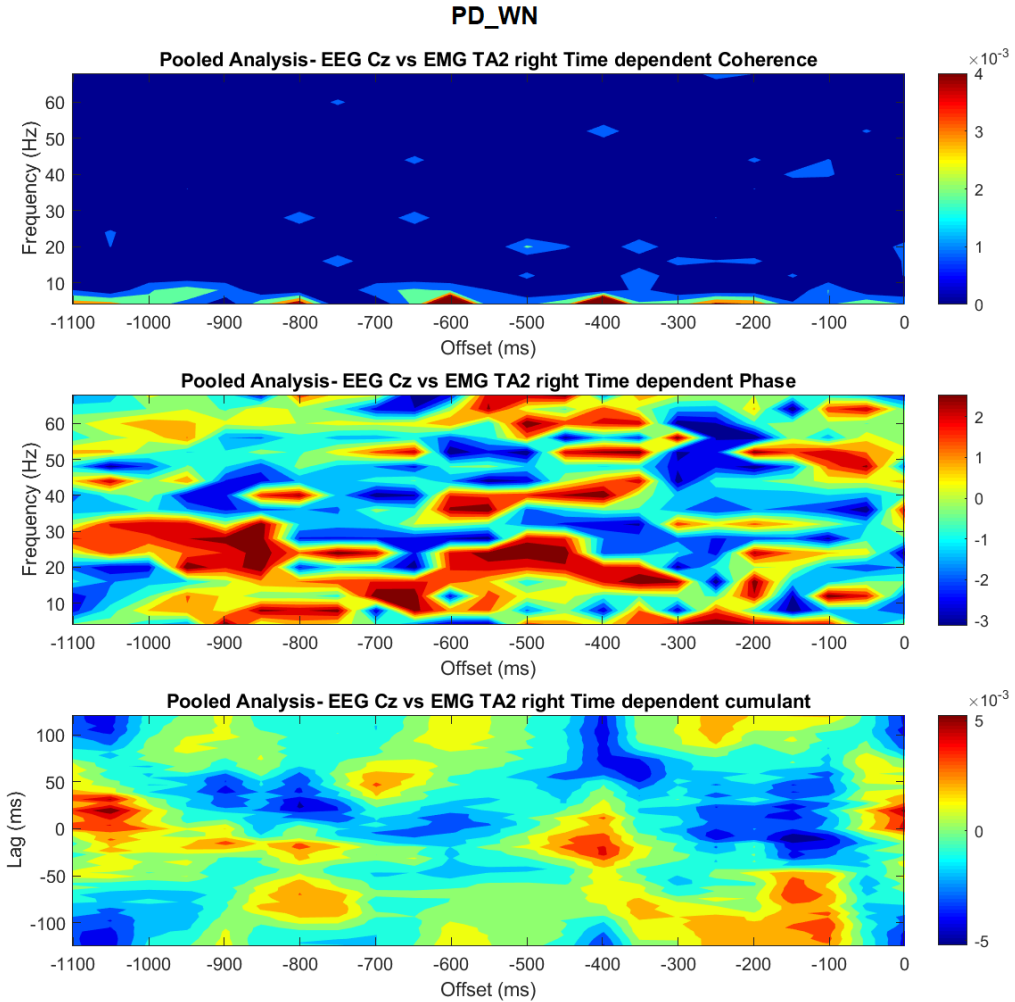


Figure 4: Shows  $T_d$  estimates of corticomuscular coupling parameters for PD\_WN, i.e. coherence (top), phase (middle), cumulant density (bottom) for cortical region Cz and muscle TA of the right leg.

Figure 5 illustrates pooled estimates of coherence, phase and cumulant density for PD\_WEA between Cz and TA. Here, significant coherence at low frequencies (2-13 Hz) is present for almost the whole gait cycle. Significant coherence in beta frequency range is present in most of the swing phase (from -400 ms to -100 ms relative to RHS). Significant coherence in gamma frequency range is present just before the RHS (-50 ms, of about 50 Hz), before LHS (-600 ms in relation to RHS, of about 40 Hz), at loading response (-1000 ms, of about 55 Hz) and at midstand (-800 ms, of about 40 Hz).

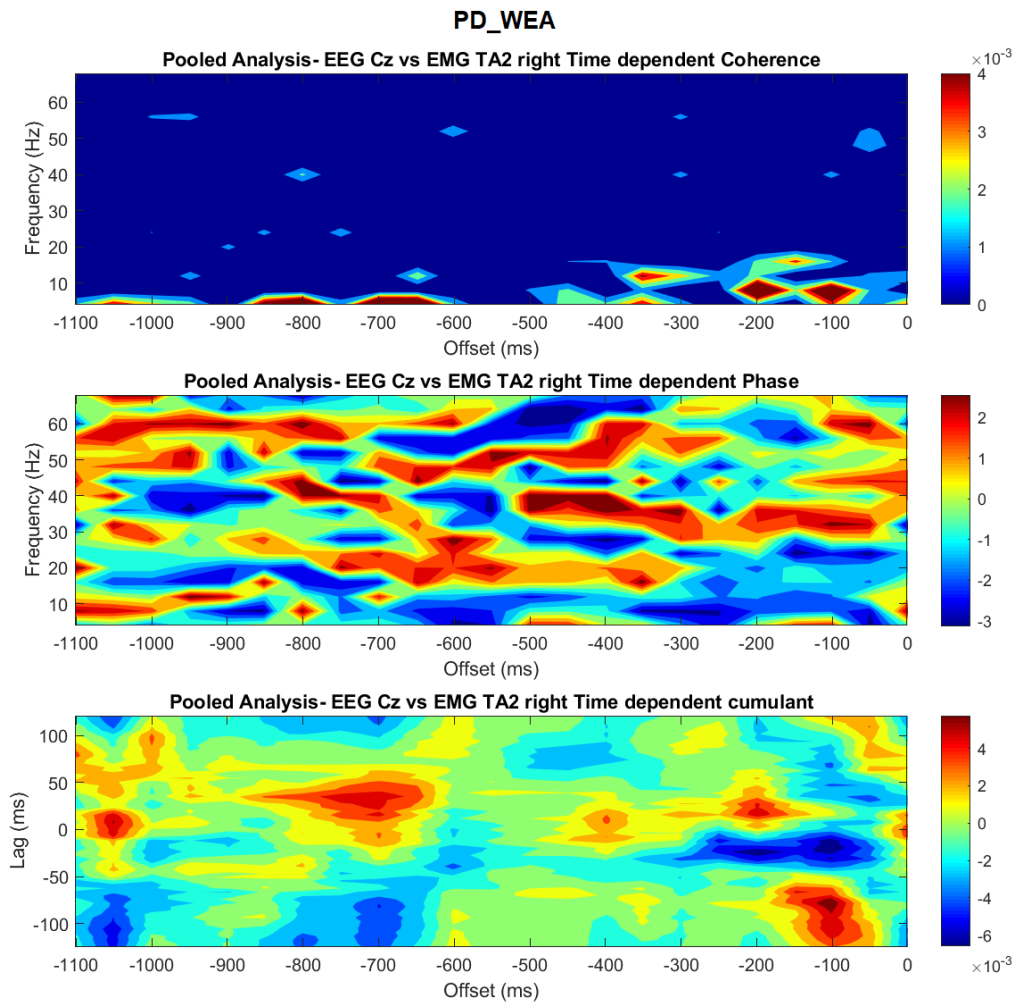


Figure 5: Shows  $T_d$  estimates of corticomuscular coupling parameters for PD\_WEA, i.e. coherence (top), phase (middle), cumulant density (bottom) for cortical region Cz and muscle TA of the right leg.

### 3.2.2 EEG data from cortical region Fz vs EMG data from TA

Figure 6 illustrates pooled estimates of coherence, phase and cumulant density for C\_WN between Fz and TA of the right leg. There is significant coherence present in low frequency region (2-13 Hz) in the stance phase (from -950 ms to 800 ms), before LHS (at -700 ms in relation to RHS), before and after heel strike i.e. initial swing and pre-swing region (from -600 to -400 ms) and, in most of the swing phase (from -300 ms to 0 ms). In beta frequency range, coherence is present at during midstand region (from -875 ms to -725 ms, of about 20 Hz), terminal stance (from -700 ms to -575 ms, of 15 Hz) and at midswing (-250 ms, of about 20 Hz).

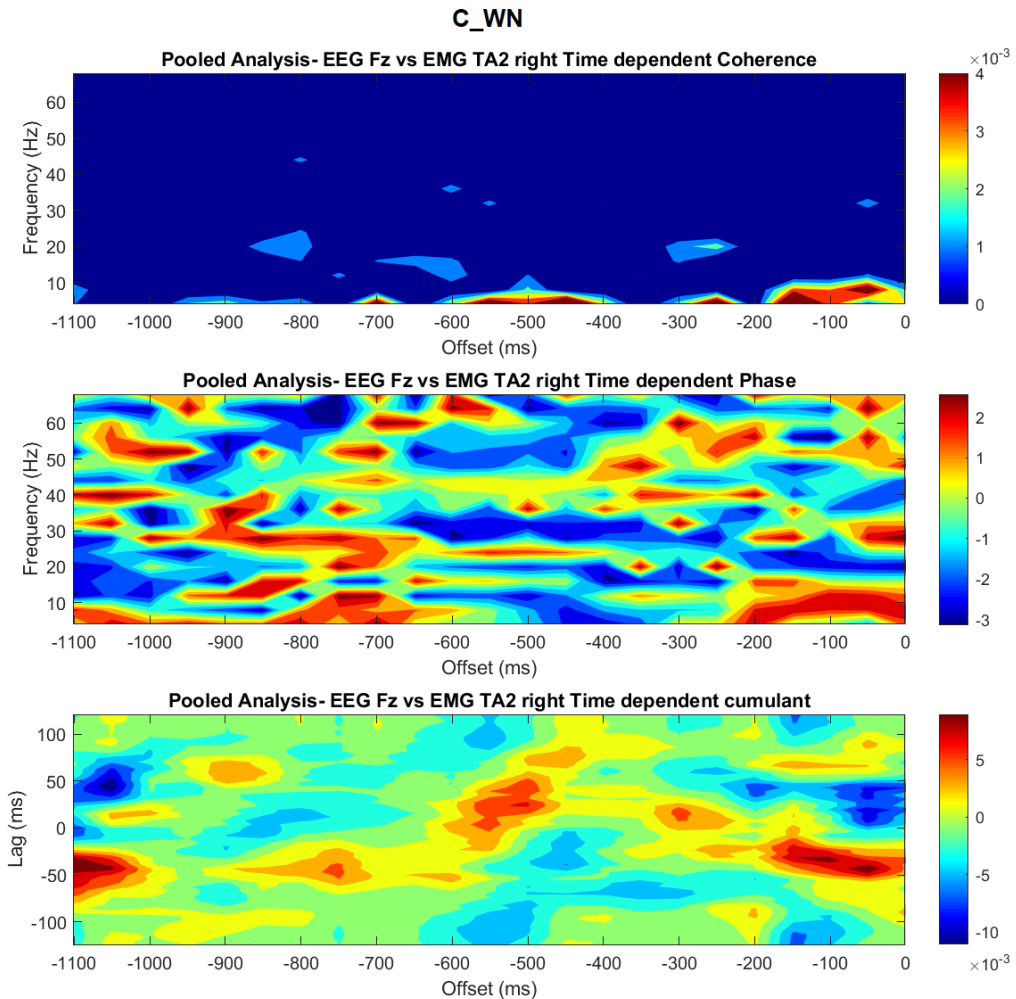


Figure 6: Shows  $T_d$  estimates of corticomuscular coupling parameters for C\_WN, i.e. coherence (top), phase (middle), cumulant density (bottom) for cortical region Fz and muscle TA of the right leg.

Figure 7 illustrates pooled estimates of coherence, phase and cumulant density for C\_WEA between Fz and TA of the right leg. Low frequency coherence is present in most of the stance phase (from -1100 ms to -700 ms), at LHS (-550 ms) and in most of the swing phase (-450ms to -100 ms). Beta frequency coherence is present just after the LHS in preswing (from -500 ms to -450 ms, of about 15 Hz) phase. Gamma band coherence is present in most of the swing phase in form of 2 peaks. One is of 55 Hz from -450 ms to -300 ms and other is of about 40 Hz from -450 ms to -300 ms in relation to the RHS. In stance phase there is one peak in gamma frequency range of about 50 Hz after the RHS at -1050 ms.

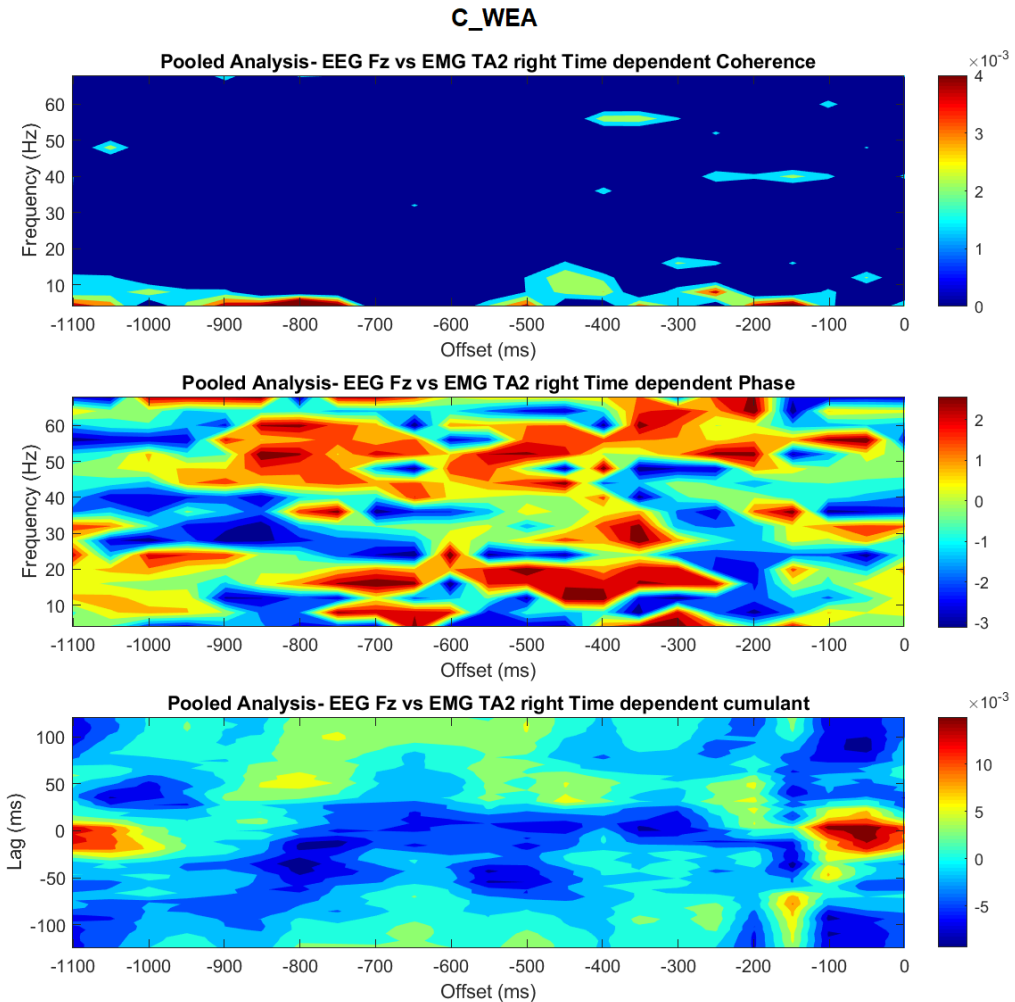


Figure 7: Shows  $T_d$  estimates of corticomuscular coupling parameters for C\_WEA, i.e. coherence (top), phase (middle), cumulant density (bottom) for cortical region Fz and muscle TA of the right leg.

Figure 8 illustrates pooled estimates of coherence, phase and cumulant density for PD\_WN between Fz and TA of the right leg. Low frequency coherence is present in the stance phase before LHS (from -900 ms to -600 ms) and in the swing phase after LHS at -450 ms and also from -150 ms to -50 ms in relation to the RHS. Beta frequency coherence of about 20 Hz is present at -450 ms and -150 ms. Gamma band coherence of 50 Hz is present at -550 ms, -400 ms and from -200 ms to -100 ms in relation to RHS.

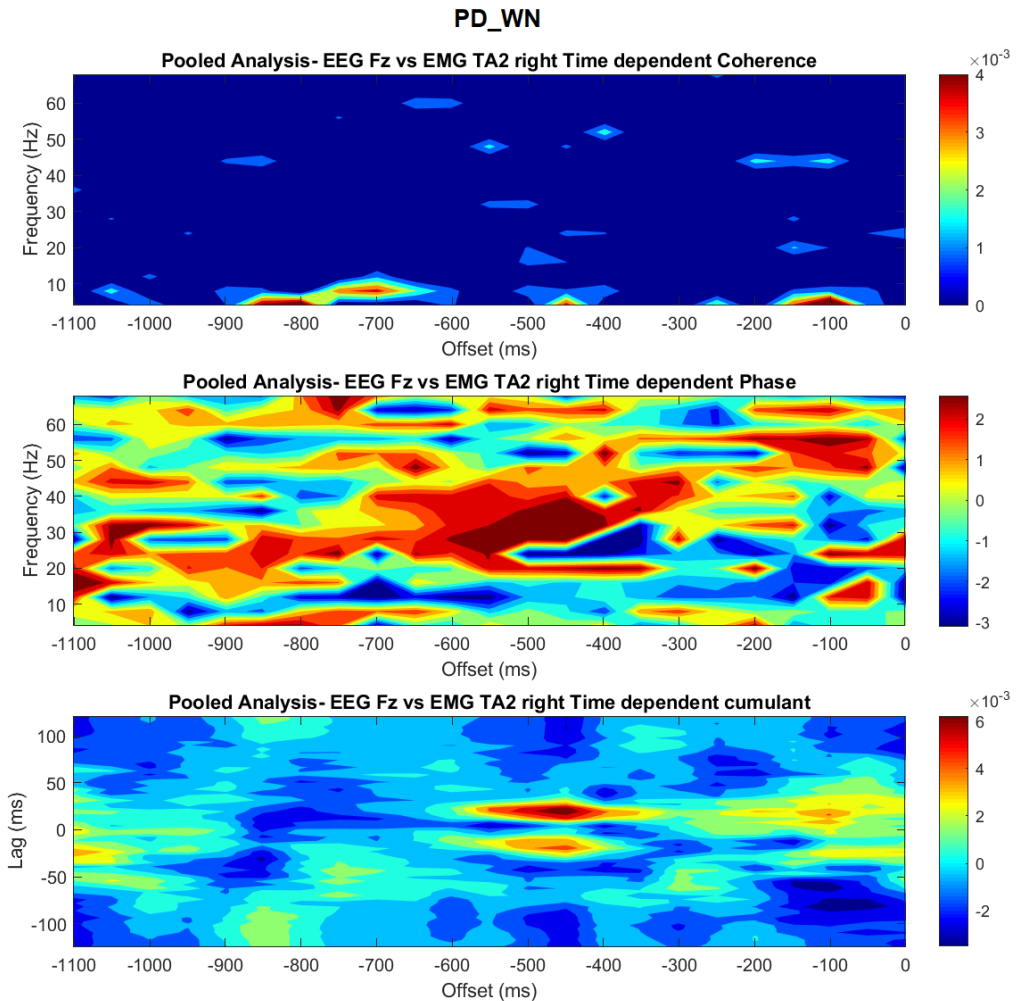


Figure 8: Shows  $T_d$  estimates of corticomuscular coupling parameters for PD\_WN, i.e. coherence (top), phase (middle), cumulant density (bottom) for cortical region Fz and muscle TA of the right leg.

Figure 9 illustrates pooled estimates of coherence, phase and cumulant density for PD\_WEA between Fz and TA of the right leg. Low frequency coherence in stance phase is present from -1050 ms to -950 ms, in swing phase it can be seen from -500 ms to -400 ms and from -250 ms to -100 ms. Significant gamma frequency coherence can be seen in form of small peaks at -1050 ms, -1000 ms, -900 ms, -750 ms, -600 ms, -350 ms and -200 ms.

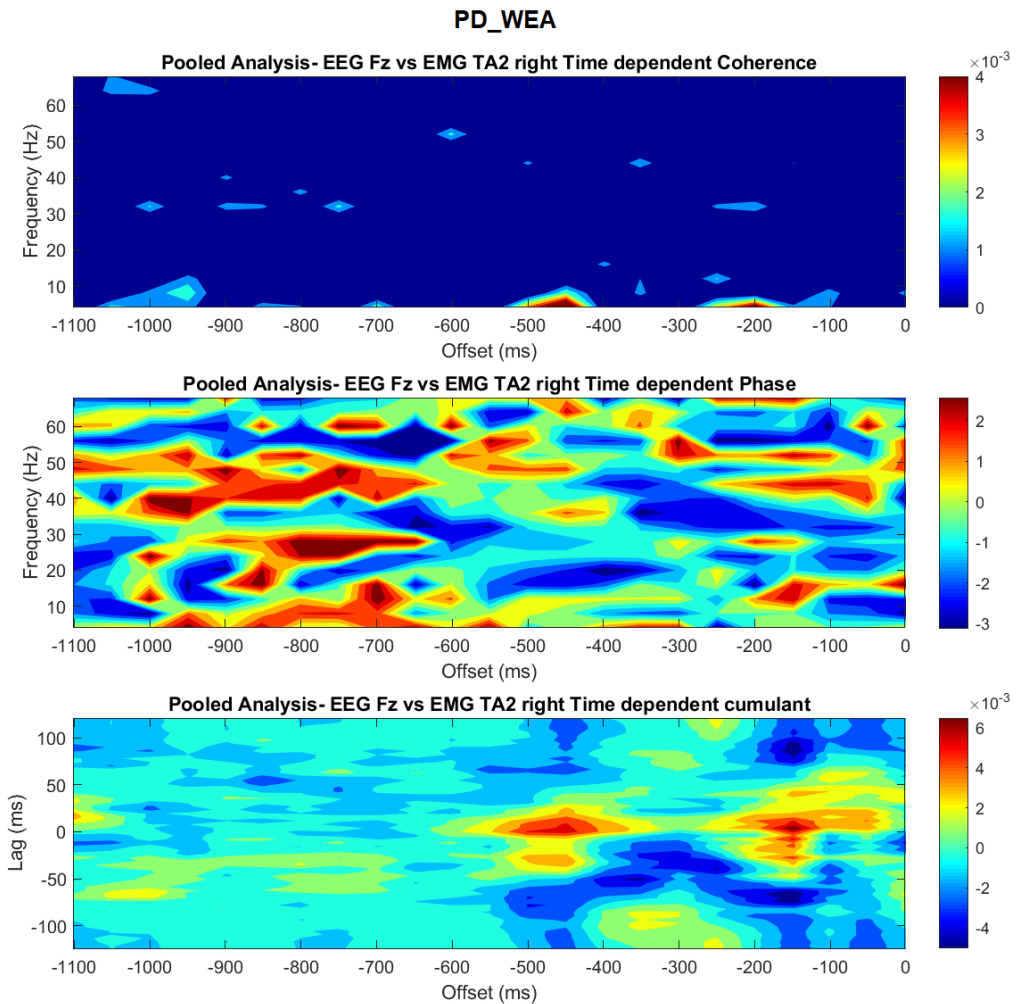


Figure 9: Shows  $T_d$  estimates of corticomuscular coupling parameters for PD\_WEA, i.e. coherence (top), phase (middle), cumulant density (bottom) for cortical region Fz and muscle TA of the right leg.

### 3.2.3 EEG data from cortical region Cz vs EMG data from RF

Figure 10 illustrates pooled estimates of coherence, phase and cumulant density for C\_WN between Cz and RF of the right leg. Low frequency coherence can be seen after RHS from initial contact to midstand (from -1050 ms to -800 ms), between terminal stance and initial swing (from -700 ms to -600 ms), between midswing and terminal swing (from -200 ms to -100 ms), and at RHS (0 ms). Gamma band coherence of about 50 Hz can be seen in stance phase from -950 ms to -750 ms and just before LHS (-600 ms in reaction to RHS).

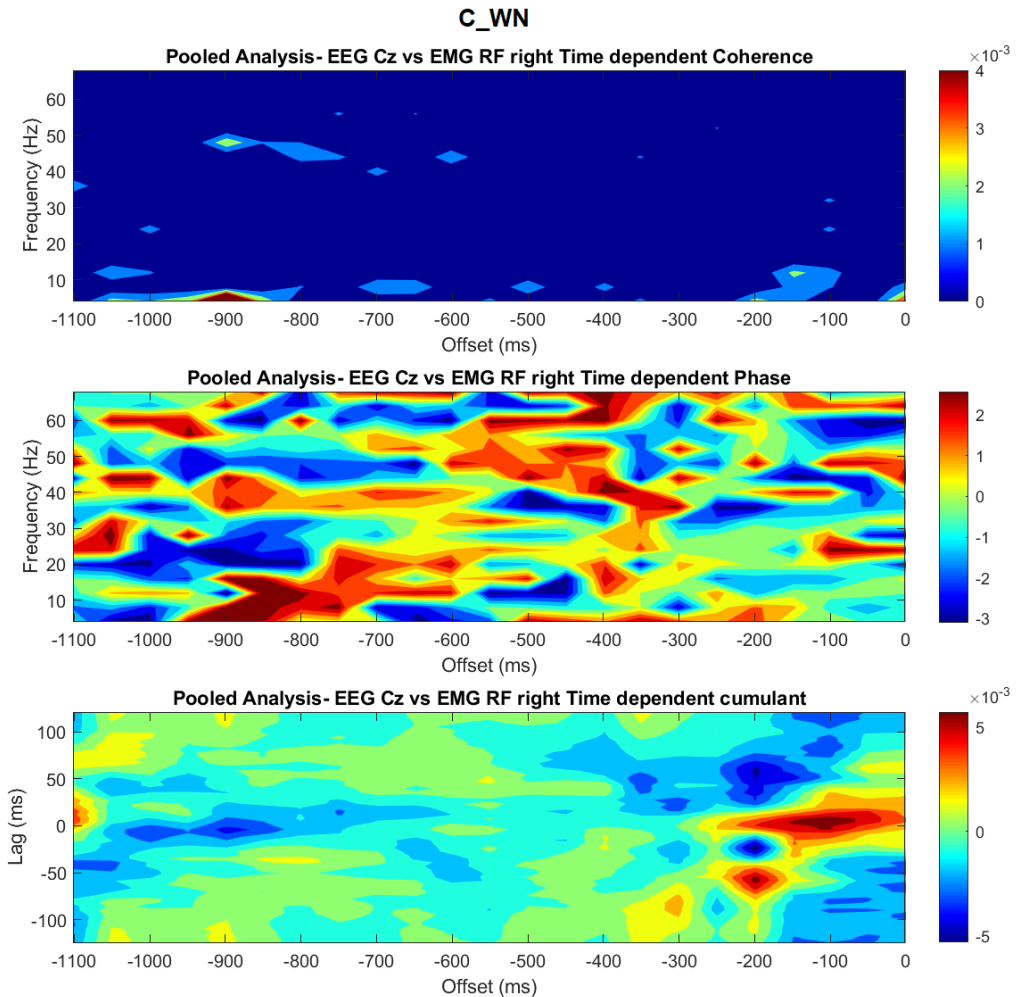


Figure 10: Shows  $T_d$  estimates of corticomuscular coupling parameters for C\_WN, i.e. coherence (top), phase (middle), cumulant density (bottom) for cortical region Cz and muscle RF of the right leg.

Figure 11 illustrates pooled estimates of coherence, phase and cumulant density for C\_WEA between Cz and RF of the right leg. Low frequency coherence is present in a major part of stance phase (from -1050 ms to -750 ms) and almost in the whole swing phase after LHS (from -550 ms to 0 ms). Beta frequency coherence of 30 Hz is present at the LHS. In stance phase, gamma band coherence is present from the loading response to the LHS (from -950 ms to -550 ms) in the frequency band from 30 to 44 Hz. One peak of gamma frequency coherence of 56 Hz is present on the LHS, two peaks of 48 Hz and 64 Hz are present at -350 ms and -250 ms, respectively, in the swing phase and one peak of 40 Hz is present at the RHS.

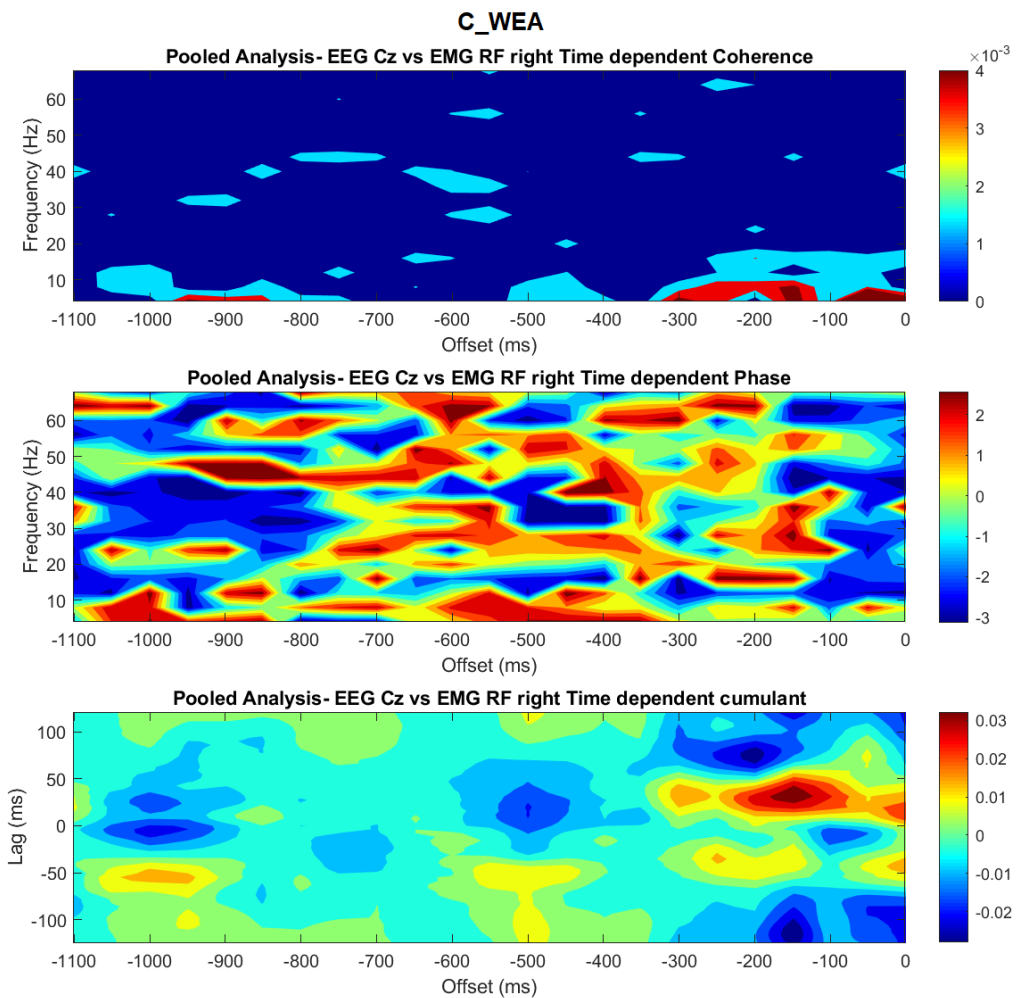


Figure 11: Shows  $T_d$  estimates of corticomuscular coupling parameters for C\_WEA, i.e. coherence (top), phase (middle), cumulant density (bottom) for cortical region Cz and muscle RF of the right leg.

Figure 12 illustrates pooled estimates of coherence, phase and cumulant density for PD\_WN between Cz and RF of the right leg. Low frequency coherence is present in almost the whole stance phase (from -1100 ms to -900 ms and from -800 ms to -550 ms) and almost the whole swing phase (from -400 ms to 0 ms). Beta frequency coherence is present during loading response (from -1000 ms to -950 ms) and a little before the LHS (at -650 ms). Gamma frequency coherence of 40 hz can be seen at -950 ms, -750 ms and -150 ms.

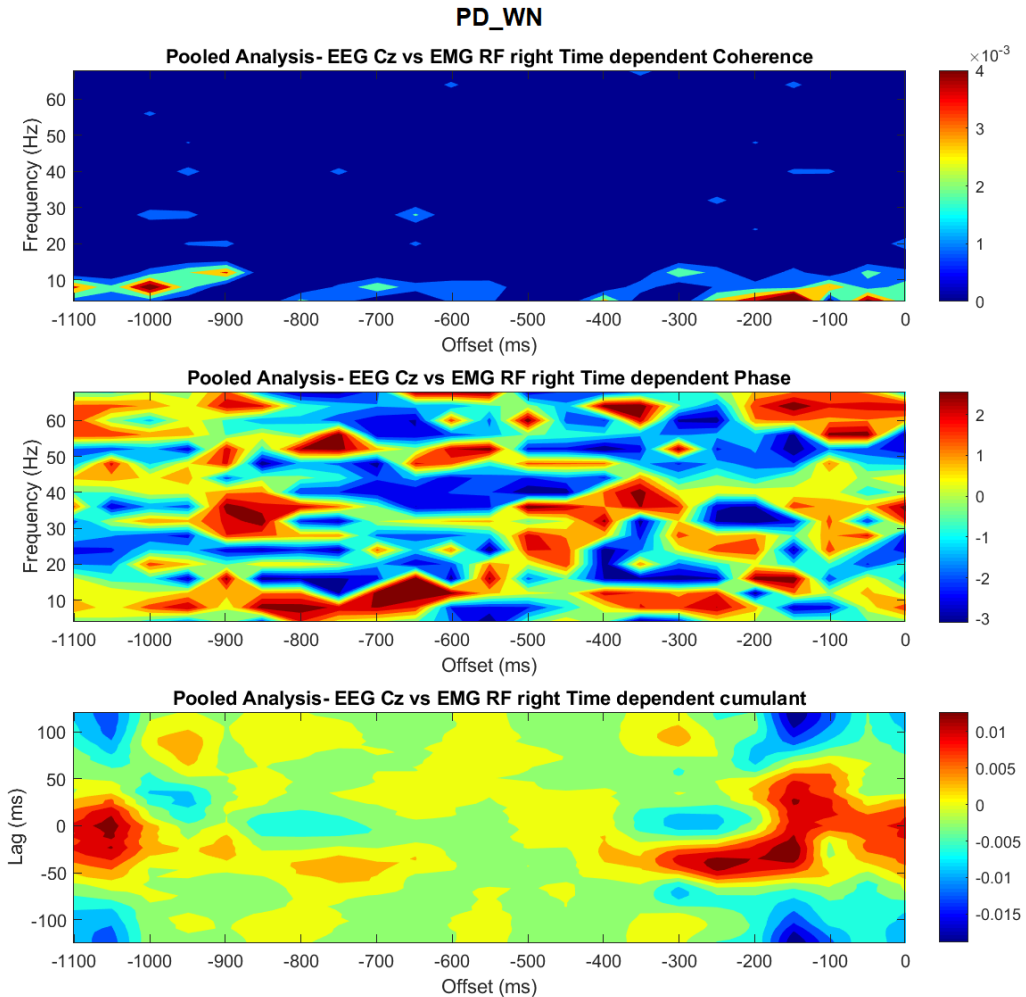


Figure 12: Shows  $T_d$  estimates of corticomuscular coupling parameters for PD\_WN, i.e. coherence (top), phase (middle), cumulant density (bottom) for cortical region Cz and muscle RF of the right leg.

Figure 13 illustrates pooled estimates of coherence, phase and cumulant density for PD\_WEA between Cz and RF of the right leg. Low frequency coherence is present in almost the whole stance phase (from -1100 ms to -850 ms and from -700 ms to -600 ms), just after the LHS (at -450 ms) and in the whole swing phase (from -400 ms to 0 ms). Beta frequency coherence of 20 Hz is present in the stance phase during loading response at -1000 ms, of 25 Hz around LHS from -650 ms to -450 ms, and in stance phase at -350 ms during preswing. Gamma frequency coherence of 50 Hz is present during terminal swing from -200 ms to -100 ms.

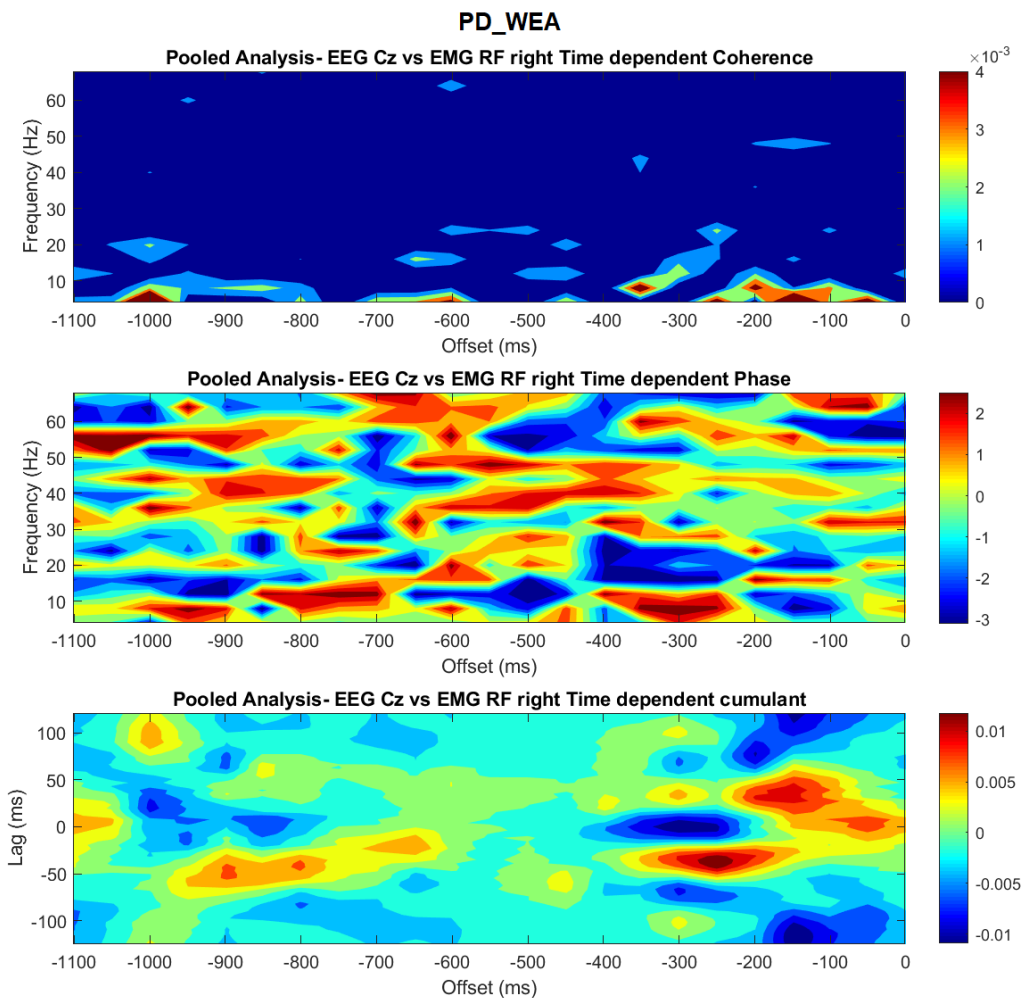


Figure 13: Shows  $T_d$  estimates of corticomuscular coupling parameters for PD\_WEA, i.e. coherence (top), phase (middle), cumulant density (bottom) for cortical region Cz and muscle RF of the right leg.

### 3.2.4 EEG data from cortical region Fz vs EMG data from RF

Figure 14 illustrates pooled estimates of coherence, phase and cumulant density for PD\_WEA between Cz and RF of the right leg. Low frequency coherence is present in the whole stance phase (from -1100 ms to -450 ms) and initial major part of swing phase (from -450 ms to -150 ms). Beta frequency coherence of 16 Hz is present at -1000 ms and of 20 Hz is present at -650 ms, -550 ms and 0 ms. Gamma frequency coherence of approximately 32 Hz is present at RHS (-1100 ms), -750 ms and -150 ms, of 50 Hz is present just after RHS at -1100 ms and of 60 Hz is present on LHS i.e. at -550 ms.

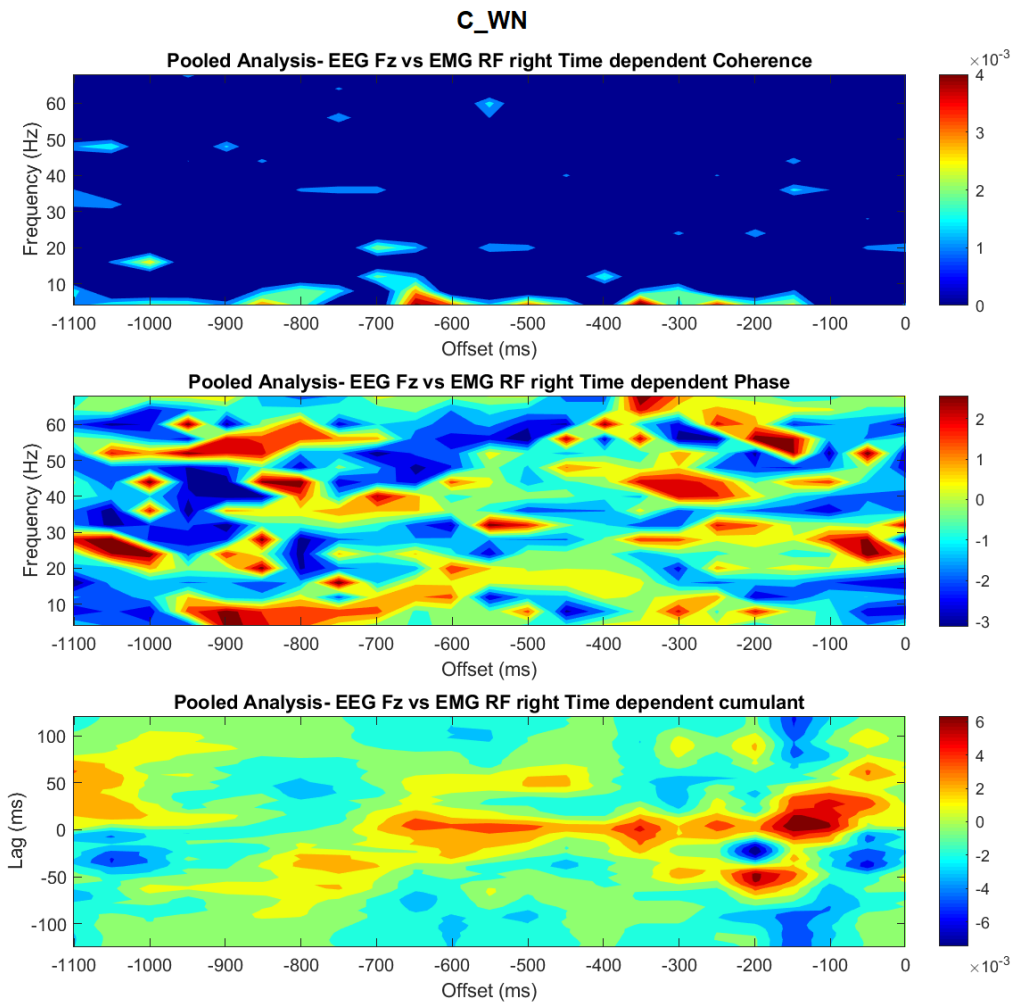


Figure 14: Shows  $T_d$  estimates of corticomuscular coupling parameters for C\_WN, i.e. coherence (top), phase (middle), cumulant density (bottom) for cortical region Fz and muscle RF of the right leg.

Figure 15 illustrates pooled estimates of coherence, phase and cumulant density for PD\_WEA between Cz and RF of the right leg. Low frequency coherence is present in the stance phase at RHS (-1100 ms), during loading response to midstand (from -950 ms to -750 ms) and in the swing phase (from -350 ms to -200 ms and from -150 ms to 0 ms). Beta frequency coherence of 18 Hz is present at two instances in stance phase (-900 ms and -700 ms). Gamma frequency coherence of 32 Hz is present at -700 ms, of 48 Hz is present at -750 ms and of 56 Hz is present at -1100 ms, -900 ms and -400 ms in relation to the RHS.

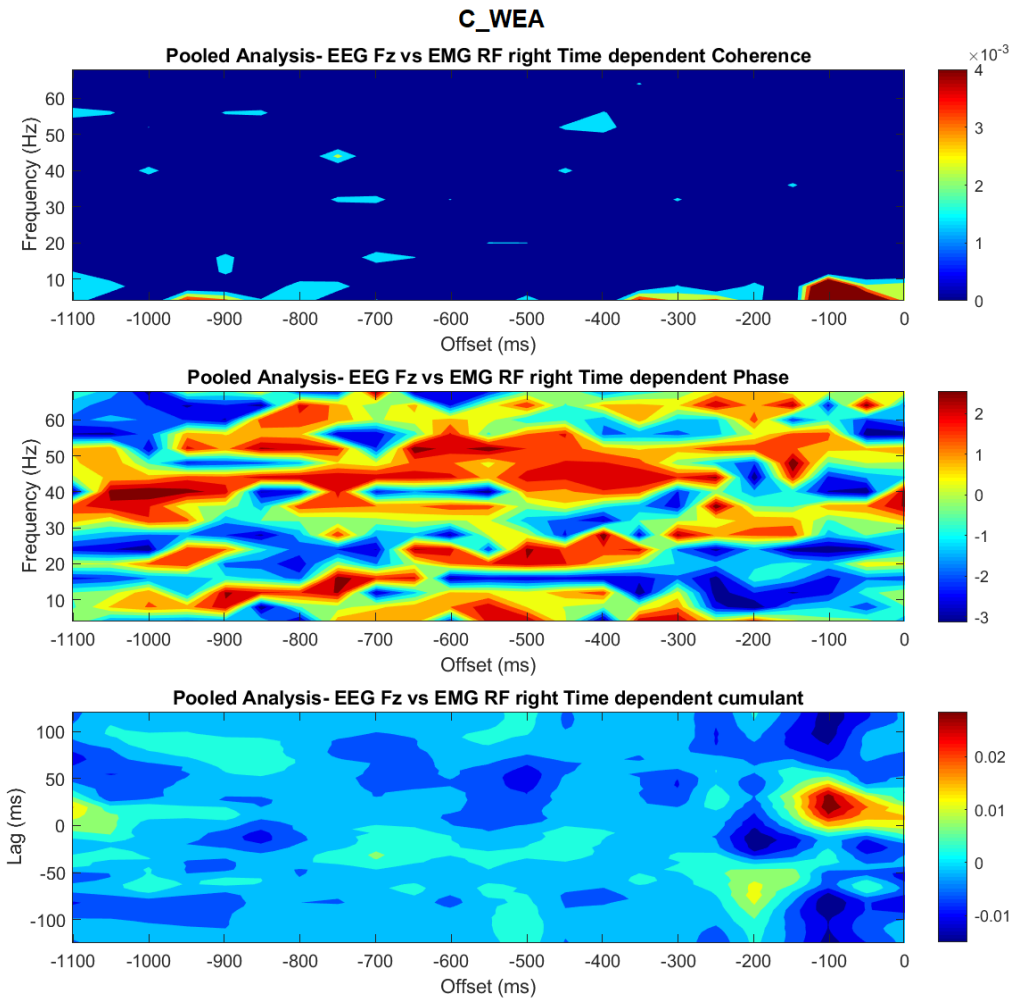


Figure 15: Shows  $T_d$  estimates of corticomuscular coupling parameters for C\_WEA, i.e. coherence (top), phase (middle), cumulant density (bottom) for cortical region Fz and muscle RF of the right leg.

Figure 16 illustrates pooled estimates of coherence, phase and cumulant density for PD\_WEA between Cz and RF of the right leg. Low frequency coherence is present in durations from -1050 ms to -950 ms and from -850 ms to -650 ms in stance phase and in swing phase at -300 ms, -150 ms and -50 ms. Beta frequency coherence of approximately 20 Hz is present before LHS form -750 ms to -600 ms. Gamma frequency coherence of 36 Hz is present in duration form -850 ms to -750 ms.

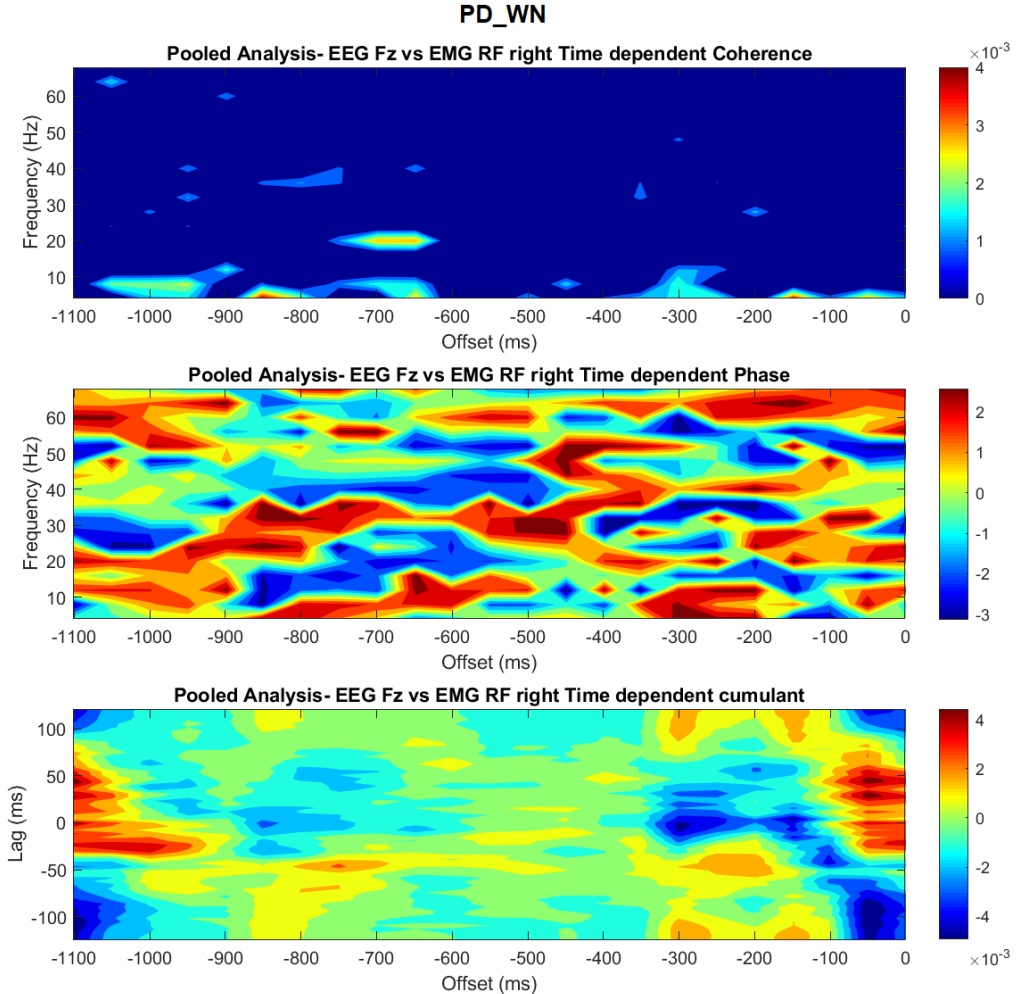


Figure 16: Shows  $T_d$  estimates of corticomuscular coupling parameters for PD\_WN, i.e. coherence (top), phase (middle), cumulant density (bottom) for cortical region Fz and muscle RF of the right leg.

Figure 17 illustrates pooled estimates of coherence, phase and cumulant density for PD\_WEA between Cz and RF of the right leg. Low frequency coherence is present in from -1000 ms to -600 ms in stance phase and in swing phase from -450 ms to -250 ms and from -150 ms to -50 ms. Beta frequency coherence of 15 Hz is present during midstance at -850 ms and of 20 Hz is present before RHS form -100 ms to 0 ms. Gamma frequency coherence of 32 Hz is present from -1000 ms to -950 ms and of 30 Hz is present just after LHS at -500 ms. One more peak of gamma frequency coherence of 50 Hz is present at -300 ms.

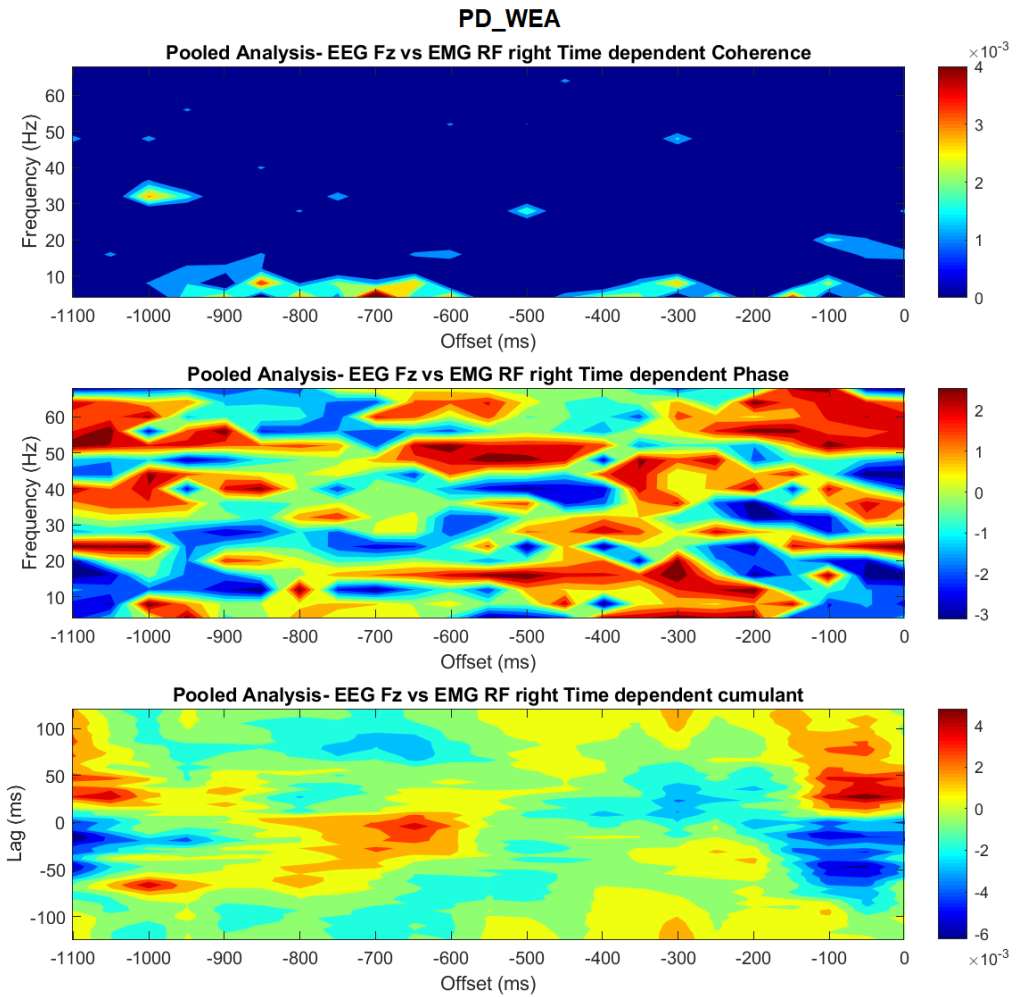


Figure 17: Shows  $T_d$  estimates of corticomuscular coupling parameters for PD\_WEA, i.e. coherence (top), phase (middle), cumulant density (bottom) for cortical region Fz and muscle RF of the right leg.

### 3.2.5 EEG data from cortical region Fz vs EMG data from DA (left)

Figure 18 illustrates pooled estimates of coherence, phase and cumulant density for C\_WN between Fz and DA of the left shoulder. Low frequency coherence is present in the end of stance phase (from -700 ms to -450 ms) and in the start of swing phase (from -450 ms to -350 ms). Further, in swing phase it can be seen as a small peak at -300 ms and as band in duration -200 ms to -100 ms. Beta frequency coherence of about 16 Hz is present from -750 ms to -650 ms, from -450 ms to -400 ms and from -200 ms to 150 ms. A strong gamma frequency coherence is present in the end of swing phase from -225 ms to -25 ms. a few peaks of gamma frequency coherence of approximately 45 Hz can also be seen at -700 ms, -600 ms, -450 ms and -350 ms.

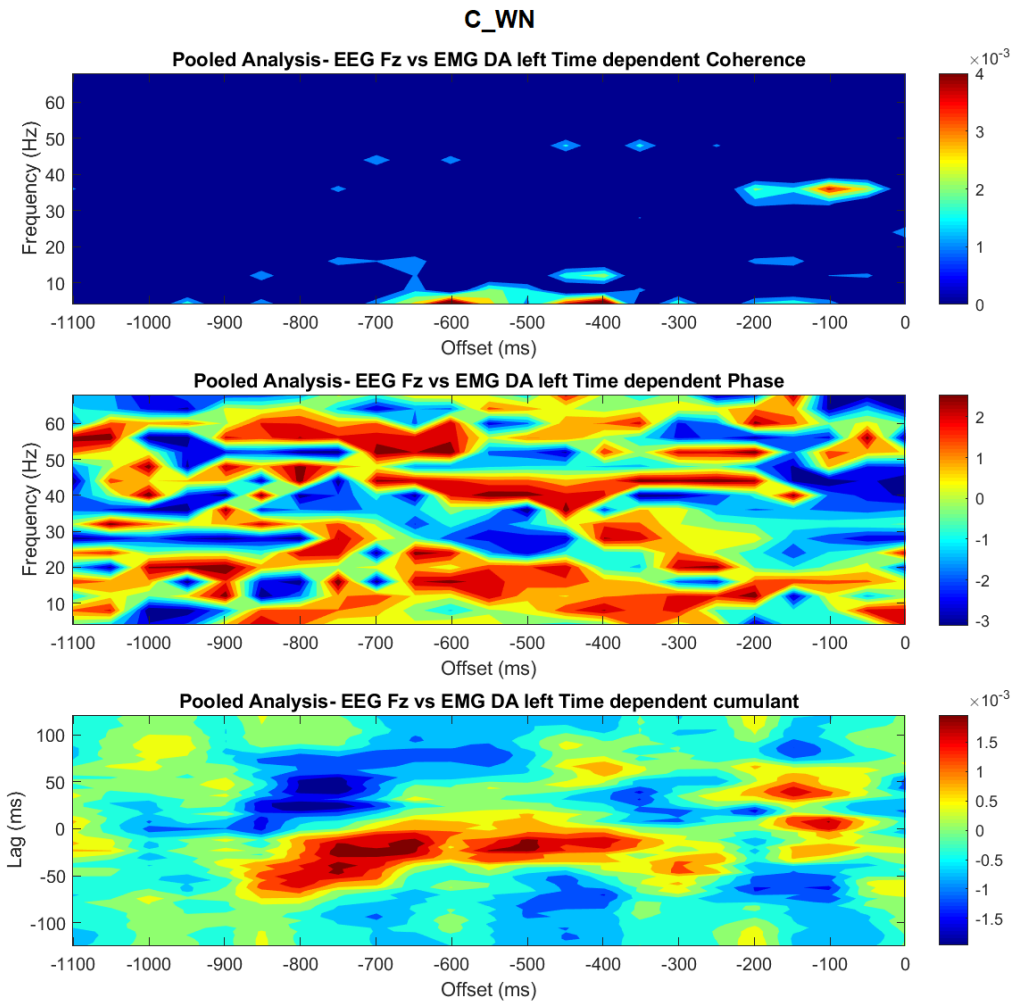


Figure 18: Shows  $T_d$  estimates of corticomuscular coupling parameters for C\_WN, i.e. coherence (top), phase (middle), cumulant density (bottom) for cortical region Fz and muscle DA of the left shoulder.

Figure 19 illustrates pooled estimates of coherence, phase and cumulant density for C\_WEA between Fz and DA of the left shoulder. Low frequency coherence is present at -1050 ms in stance phase, just after the RHS. In swing phase it can be seen from -200 ms to -100 ms and just before the RHS from -100 ms to 0 ms. Beta frequency coherence of 16 to 24 Hz is present in stance phase after RHS from -1100 ms to 950 ms, in swing phase it is evident in form of two peaks of approximately 18 Hz at -350 ms and -100 ms. Gamma frequency coherence of 32 Hz is present after RHS from -1050 ms to -900 ms, of 40 Hz at -1000 ms, of 34 Hz at LHS (-550 ms) and of 65 Hz is present from -500 ms to -400 ms in relation to the RHS.

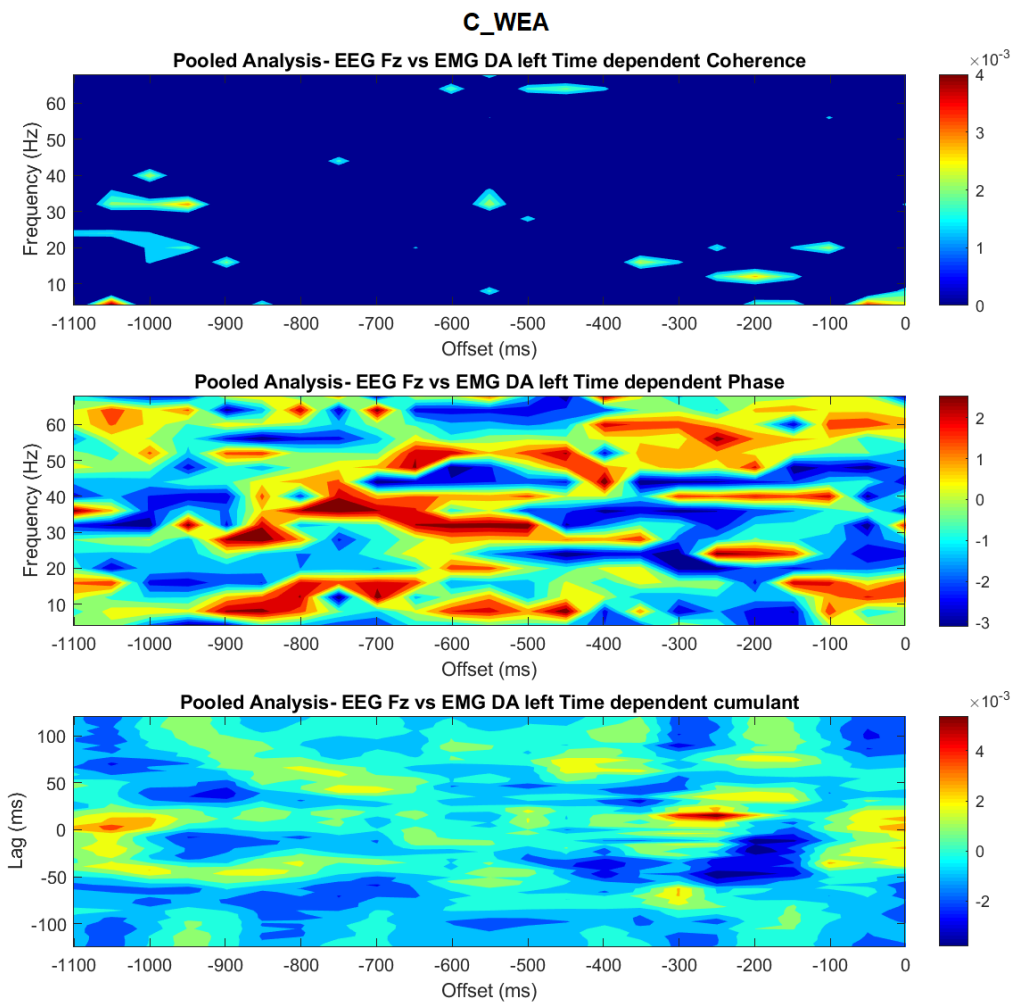


Figure 19: Shows  $T_d$  estimates of corticomuscular coupling parameters for C\_WEA, i.e. coherence (top), phase (middle), cumulant density (bottom) for cortical region Fz and muscle DA of the left shoulder.

Figure 20 illustrates pooled estimates of coherence, phase and cumulant density for PD\_WN between Fz and DA of the left shoulder. Low frequency coherence is present after the RHS from -1050 ms to -1000 ms, at -650 ms, -500 ms, -250 ms, -150 ms and at RHS (0 ms). Beta frequency coherence of 18 Hz is present at LHS (-550 ms) and of approximately 25 Hz at -450 ms, -400 ms and -150 ms. Gamma frequency coherence of 60 Hz is present after RHS from -1050 ms to -950 ms, of 40 Hz at -1000 ms, of 35 Hz at -850 ms and of 52 Hz is present from -500 ms to -450 ms.

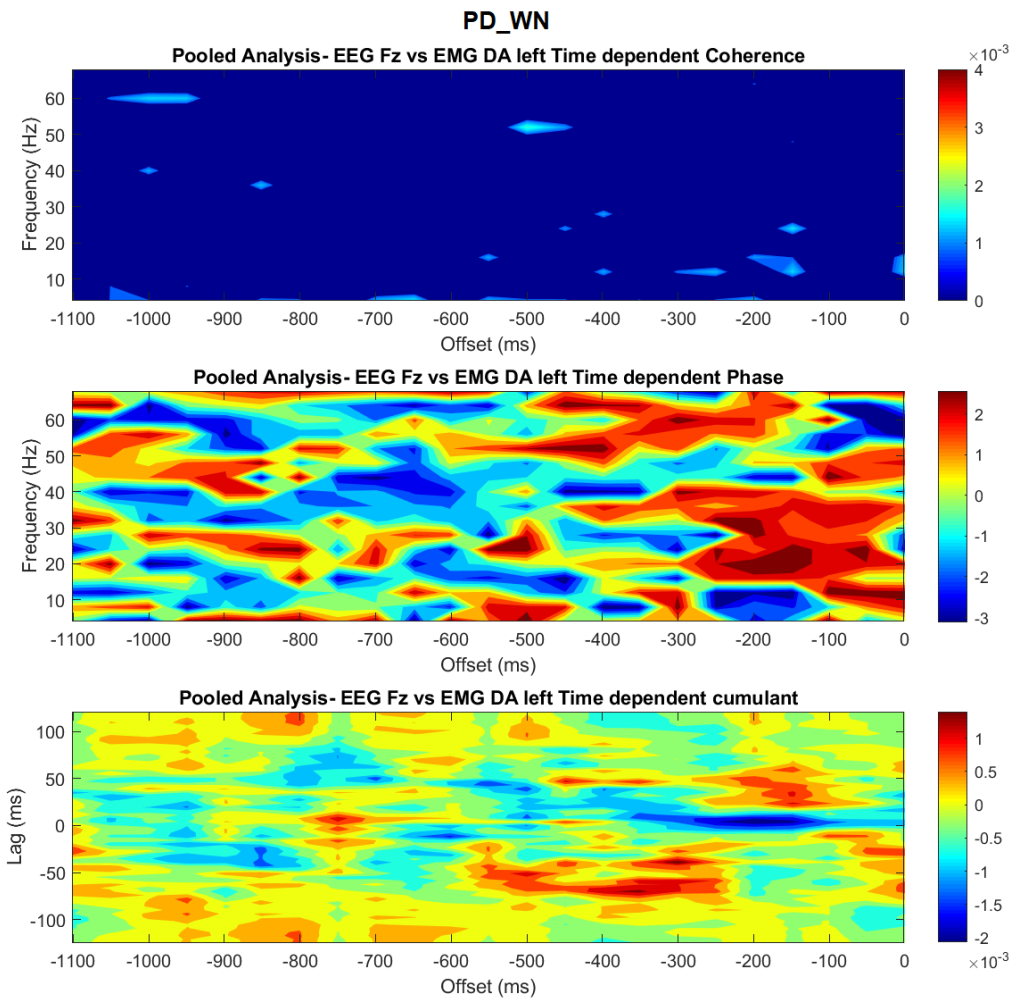


Figure 20: Shows  $T_d$  estimates of corticomuscular coupling parameters for PD\_WN, i.e. coherence (top), phase (middle), cumulant density (bottom) for cortical region Fz and muscle DA of the left shoulder.

Figure 21 illustrates pooled estimates of coherence, phase and cumulant density for PD\_WEA between Fz and DA of the left shoulder. Low frequency coherence is present from -900 ms to -850 ms in stance phase and at -400 ms, -250 ms, -150 ms is present in the swing phase. Beta frequency coherence of 20 Hz is present at -900 ms. Gamma frequency coherence is present just before the LHS from -650 ms to -600 ms, of 35 Hz and 45 Hz is present in midswing region (from -250 ms to -200 ms) and of 50 Hz is present just before the RHS at -50 ms.

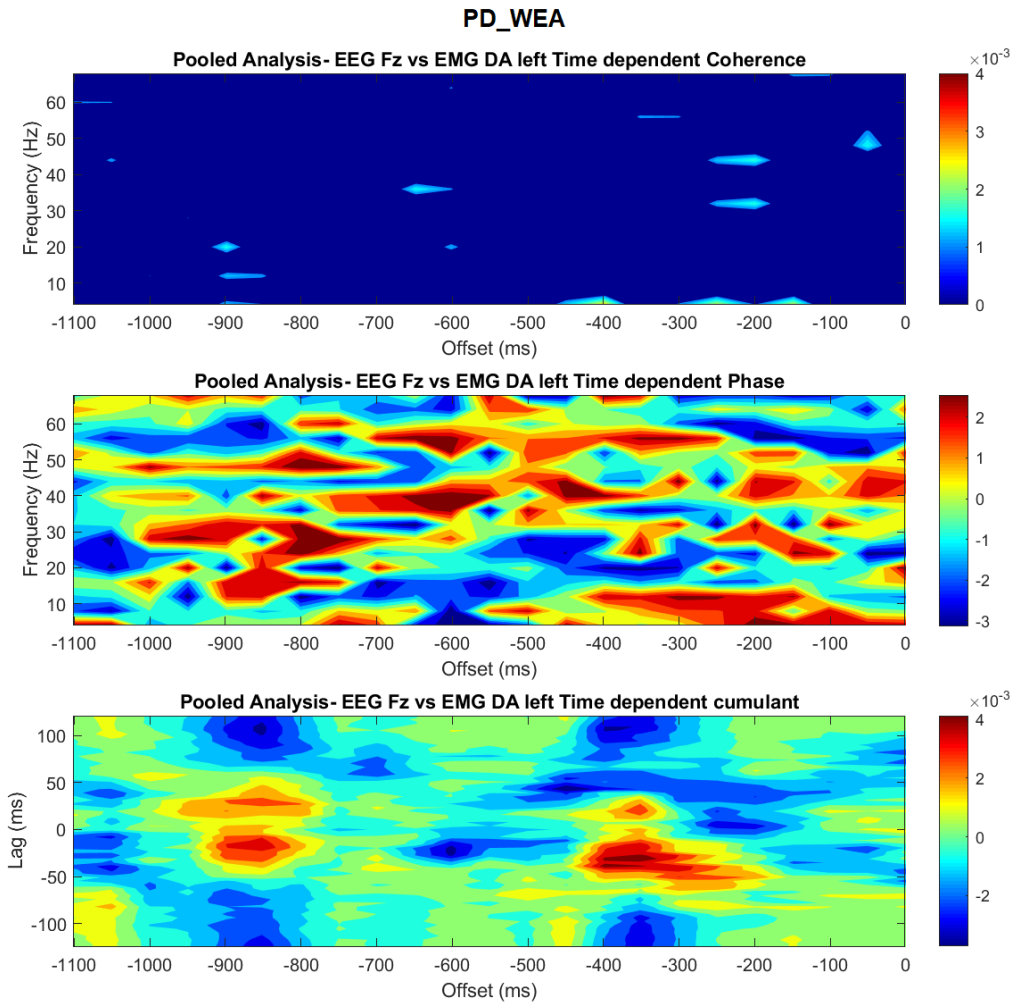


Figure 21: Shows  $T_d$  estimates of corticomuscular coupling parameters for PD\_WEA, i.e. coherence (top), phase (middle), cumulant density (bottom) for cortical region Fz and muscle DA of the left shoulder.

### 3.2.6 EEG data from cortical region C4 vs EMG data from DA (left)

Figure 22 illustrates pooled estimates of coherence, phase and cumulant density for C\_WN between C4 and DA of the left shoulder. Low frequency coherence is present after RHS (from -1100 ms to -950 ms), at -800 ms, before LHS from -700 ms to -675 ms in the stance phase and further can be seen in the whole swing phase from -450 ms to 0 ms. Beta frequency coherence of approximately 28 Hz is present just during the terminal swing at -100 ms. Gamma frequency coherence of 50-60 Hz is present before and after midstand from -900 ms to -700 ms, of 40Hz at LHS and of 45 Hz is present before the RHS from -125 ms to -25 ms.

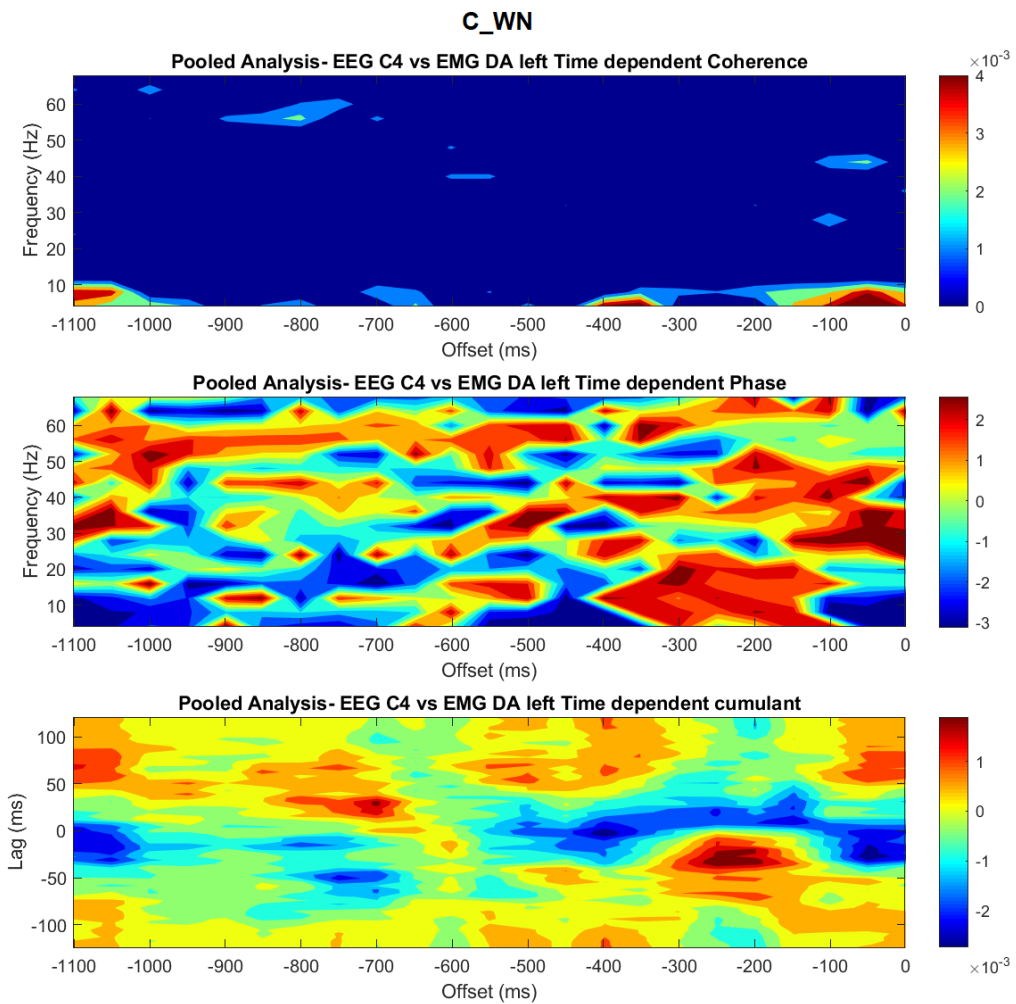


Figure 22: Shows  $T_d$  estimates of corticomuscular coupling parameters for C\_WN, i.e. coherence (top), phase (middle), cumulant density (bottom) for cortical region C4 and muscle DA of the left shoulder.

Figure 23 illustrates pooled estimates of coherence, phase and cumulant density for C\_WEA between Cz and DA of the left shoulder. Low frequency coherence is present after the RHS from -1100 ms to -1000 ms and at -800 ms in stance phase. In swing phase it can be seen from -350 ms to -75 ms and from -25 ms to 0 ms before the RHS. Beta frequency coherence of 20 Hz is present after midstand from -750 ms to -675 ms and of approximately 25 Hz at -350 ms. Gamma frequency coherence of 35 Hz is present at LHS (-550 ms), of 50 Hz can be seen after LHS from -550 ms to -500 ms, of 45 Hz at -450 ms, of 35 Hz before the RHS at -100 ms and of 40 Hz is present at -50 ms.

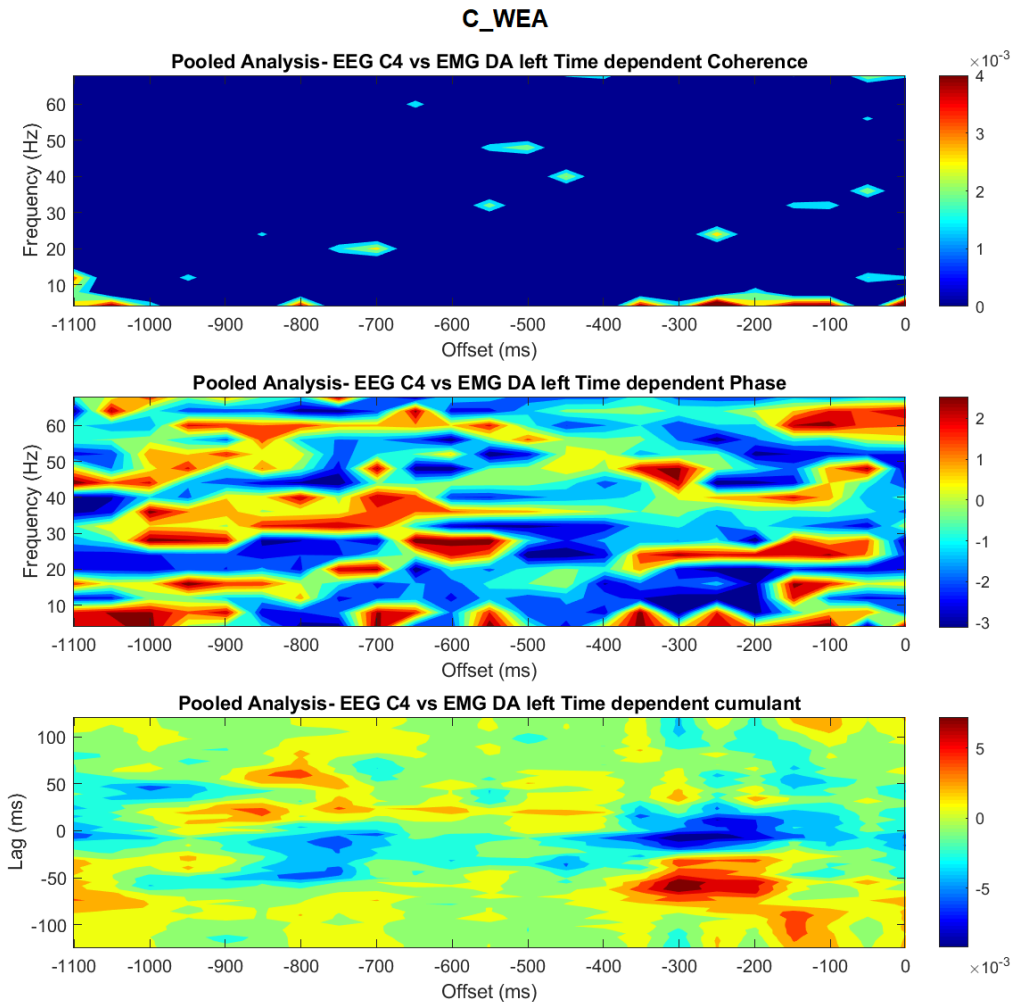


Figure 23: Shows  $T_d$  estimates of corticomuscular coupling parameters for C\_WEA, i.e. coherence (top), phase (middle), cumulant density (bottom) for cortical region C4 and muscle DA of the left shoulder.

Figure 24 illustrates pooled estimates of coherence, phase and cumulant density for PD\_WN between Cz and DA of the left shoulder. Low frequency coherence in stance phase is present after RHS from -1075 ms to -950 ms and before LHS at -650 ms. In swing phase it is present at -400 ms, from -300 ms to -250 ms, and at -150 ms. Beta frequency coherence of 20 Hz is present at LHS. Gamma frequency coherence of 40 Hz is present in stance phase from -850 ms to -800 ms, of 55 Hz just before the LHS and of 30-35 Hz is present in the swing phase from -275 ms to -125 ms.

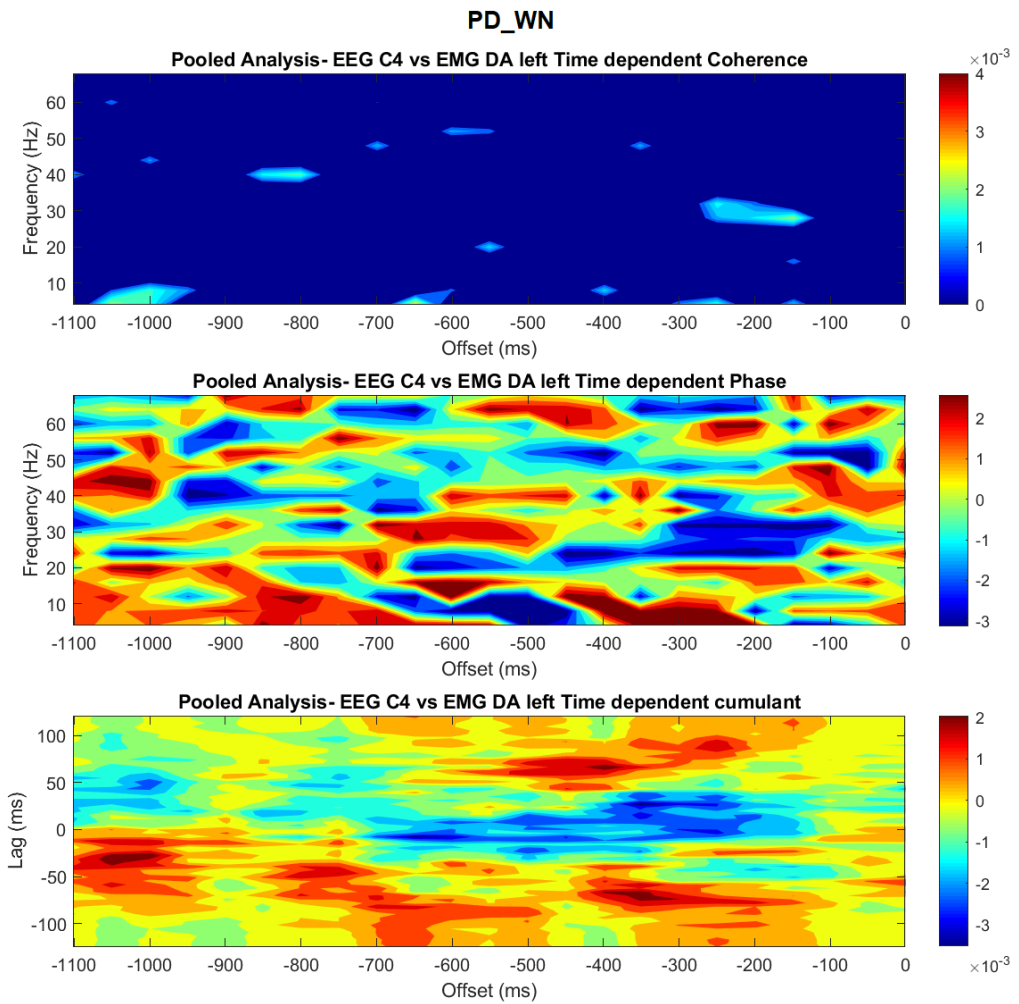


Figure 24: Shows  $T_d$  estimates of corticomuscular coupling parameters for PD\_WN, i.e. coherence (top), phase (middle), cumulant density (bottom) for cortical region C4 and muscle DA of the left shoulder.

Figure 25 illustrates pooled estimates of coherence, phase and cumulant density for PD\_WEA between Cz and DA of the left shoulder. Low frequency coherence is present at midstand (-850 ms) and after LHS from -500 ms to -450 ms in the stance phase. In the swing phase it can be seen from -150 ms to -100 ms. Beta frequency coherence of 20 Hz is present after the midstand from -800 ms to -750 ms, of 18 Hz is present at -450 ms and from -150 ms to -100 ms. Gamma frequency coherence of 56 Hz is present at LHS (-550 ms) and a little before the LHS (-650 ms).

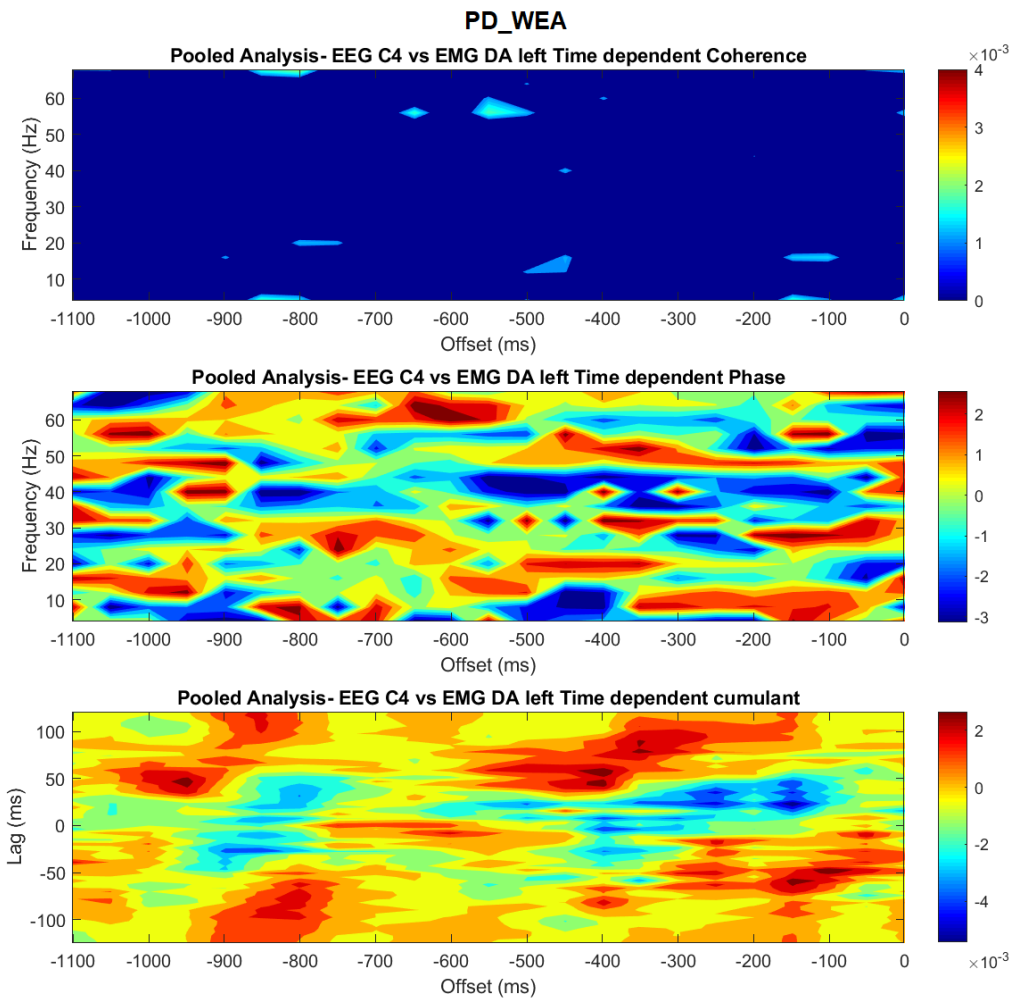


Figure 25: Shows  $T_d$  estimates of corticomuscular coupling parameters for PD\_WEA, i.e. coherence (top), phase (middle), cumulant density (bottom) for cortical region C4 and muscle DA of the left shoulder.

### 3.3 Comparison of Coherence

After calculating the pooled estimates of coherence, phase and cumulant density, the difference of coherence between the four groups were calculated. The difference in coherence describes how the control group is different from the Parkinson's disease group and how enhanced arm swing during walking is different from the walking normally. In comparison of coherence, spots which have a color more towards blue spectrum of colorbar indicate that the 2<sup>nd</sup> group in the comparison has more coherence and more towards red spectrum indicates that the 1<sup>st</sup> group in the comparison has more coherence.

**Cz vs TA:** While comparing (figure 26), it can be observed that C\_WN has more coherence than C\_WEA. Also, PD\_WEA has more coherence than PD\_WN except during midstand. While comparing C\_WN to PD\_WN, PD\_WN has more coherence except at LHS. When comparing C\_WN and PD\_WEA it can be observed that the coherence difference at midstand between PD\_WN and PD\_WEA is vanished in this case.

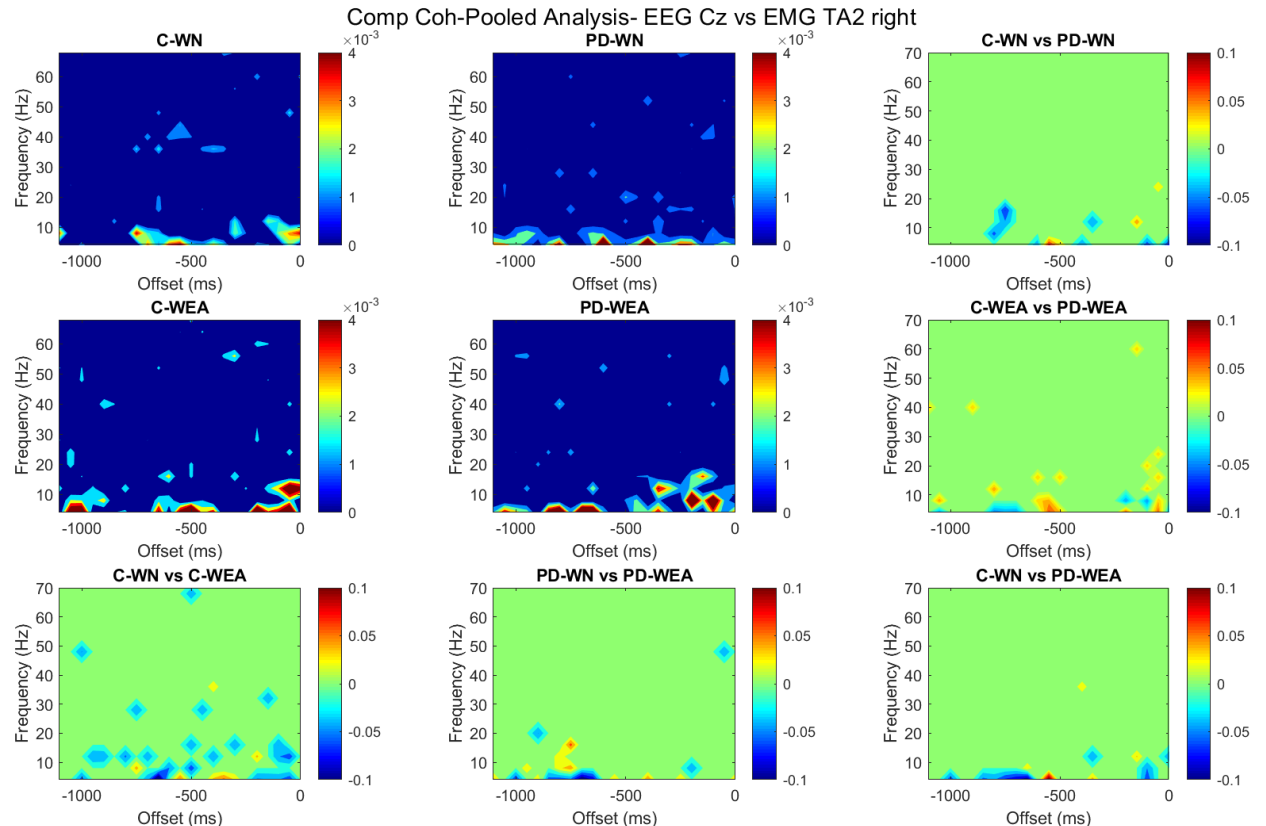


Figure 26: Shows  $T_d$  comparison of coherences for the four groups for cortical region Cz and muscle TA of the right leg.

**Fz vs TA:** While comparing (figure 27), it can be observed that C\_WEA has more coherence than C\_WN. When comparing while in PD\_WN with PD\_WEA, in swing phase PD\_WEA has more coherence than PD\_WN and during LHS and stance phase PD\_WN has more coherence than PD\_WEA. While comparing C\_WN to PD\_WN, it can be observed that PD\_WN has more coherence which is present just after the LHS and spread in end of the beta and start of the gamma frequency range. While comparing C\_WN to PD\_WEA, the beta and gamma coherence that was present in comparison of C\_WN vs PD\_WN comparison is vanished in this comparison.

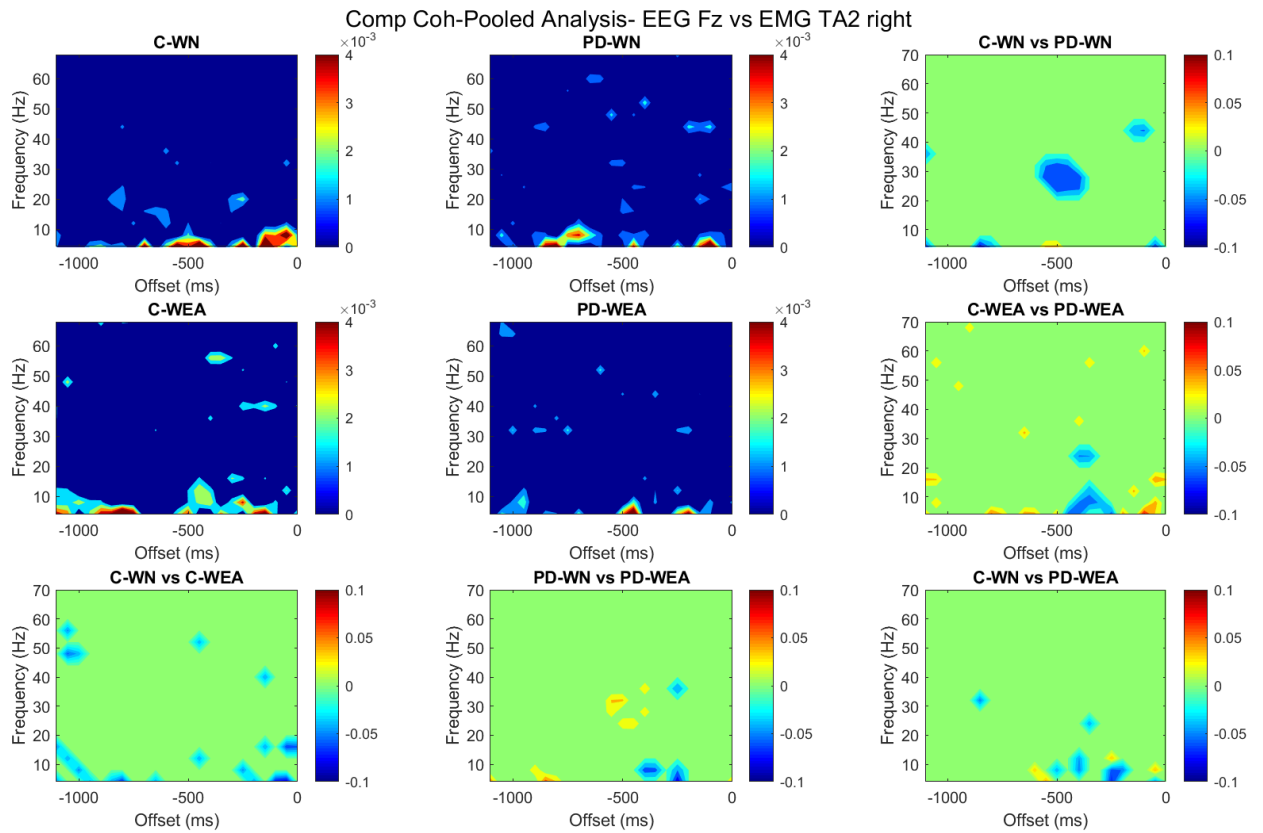


Figure 27: Shows  $T_d$  comparison of coherences for the four groups for cortical region Fz and muscle TA of the right leg.

**Cz vs RF:** While comparing (figure 28), it can be observed that C\_WEA has more coherence than C\_WN. When comparing PD\_WN to PD\_WEA, more coherence can be observed in PD\_WEA but, at some peaks, in low frequency and beta frequency range PD\_WN has more coherence than PD\_WEA. While comparing C\_WN to PD\_WN, more coherence can be seen in PD\_WN. When comparing C\_WN with PD\_WEA, the extra low frequency and beta frequency coherence in PD\_WN is vanished in this comparison.

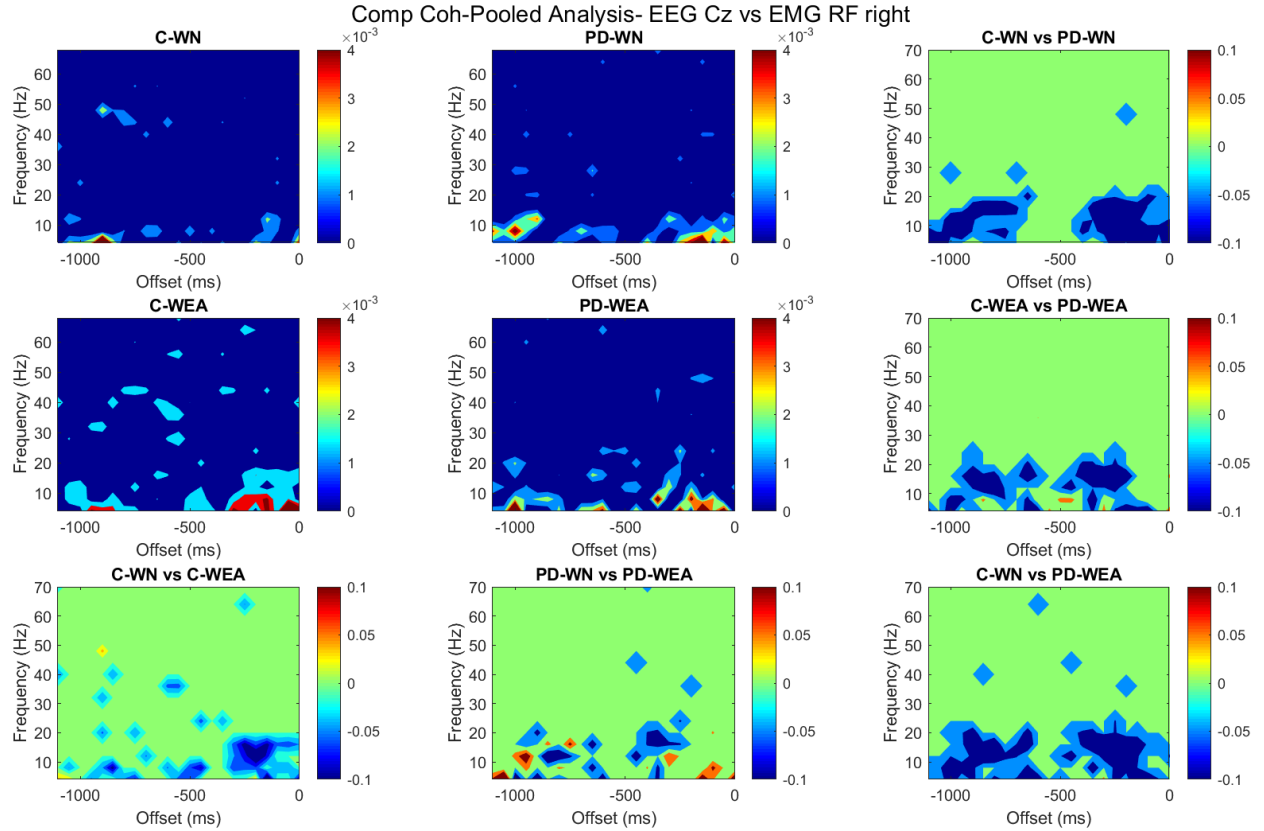


Figure 28: Shows  $T_d$  comparison of coherences for the four groups for cortical region Cz and muscle RF of the right leg.

**Fz vs RF:** While comparing (figure 29), it can be observed that PD\_WN has more coherence than C\_WN except at LHS. PD\_WEA has more coherence than PD\_WN except at some points during midswing and RHS. While comparing C\_WN to PD\_WEA, PD\_WEA has more coherence than C\_WN in stance phase and in swing phase during RHS. Also, it can be observed that PD\_WN vs PD\_WEA and C\_WN vs PD\_WEA have similar variation during midswing in low frequency and beta frequency region.

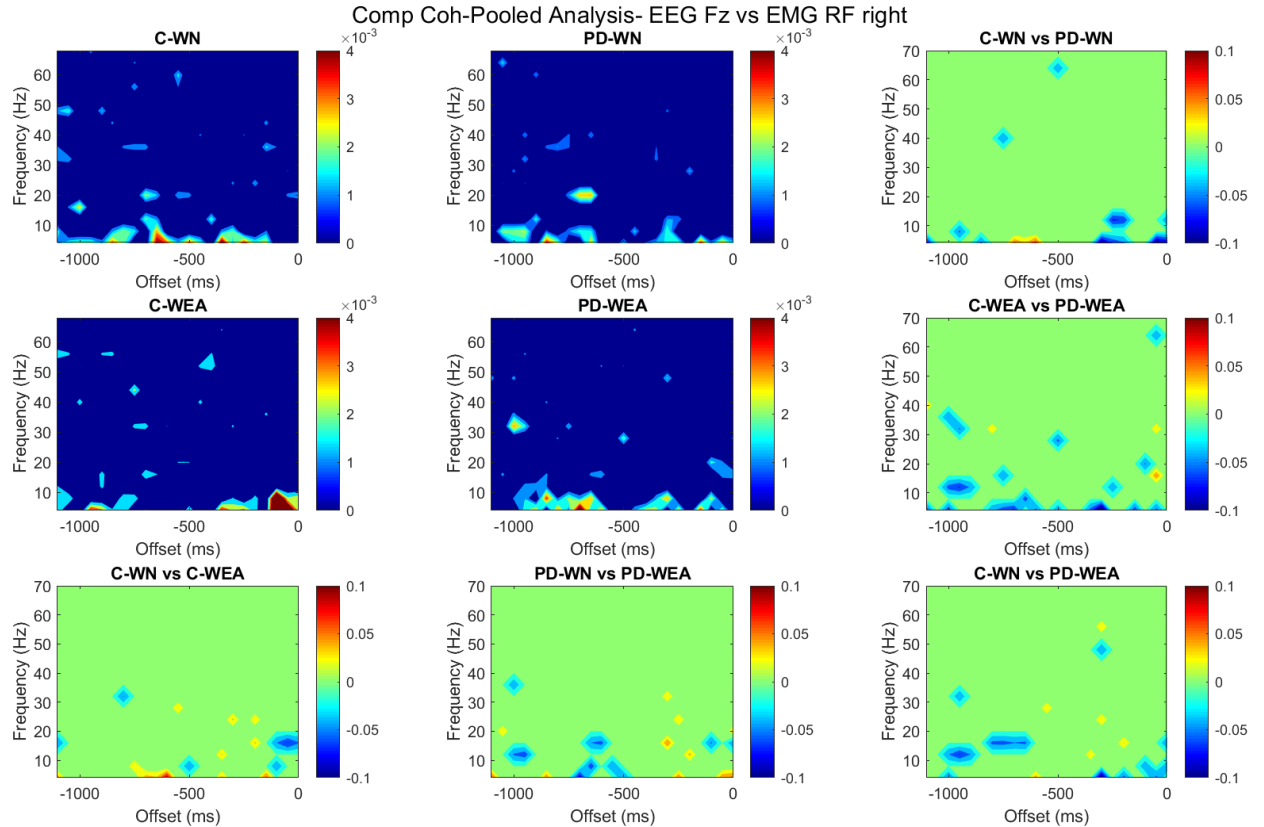


Figure 29: Shows  $T_d$  comparison of coherences for the four groups for cortical region Fz and muscle RF of the right leg.

**Fz vs DA:** While comparing (figure 30), It can be observed that C\_WN has more coherence than PD\_WN except at a point in gamma frequency range just before midstand. PD\_WN and PD\_WEA are not much different but PD\_WEA has extra theta, beta and gamma coherence in preswing region. While comparing C\_WN with PD\_WEA, only the gamma coherence just before midstand is reduced.

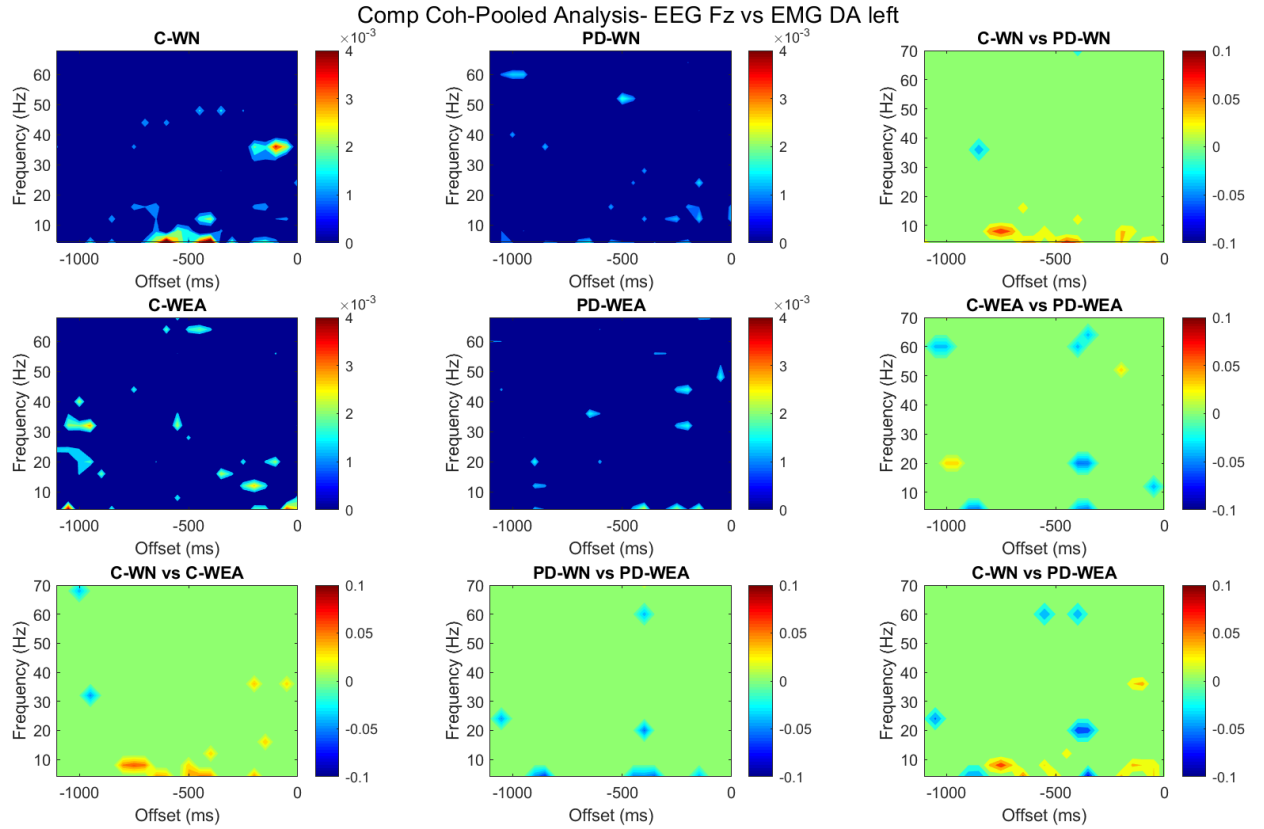


Figure 30: Shows  $T_d$  comparison of coherences for the four groups for cortical region Fz and muscle DA of the left shoulder.

**C4 vs DA:** While comparing (figure 31), it can be observed that C\_WN vs PD\_WEA is almost similar to C\_WN vs C\_WEA except the gamma coherence at LHS is vanished and PD\_WEA has more coherence at RHS in C\_WN vs PD\_WEA.

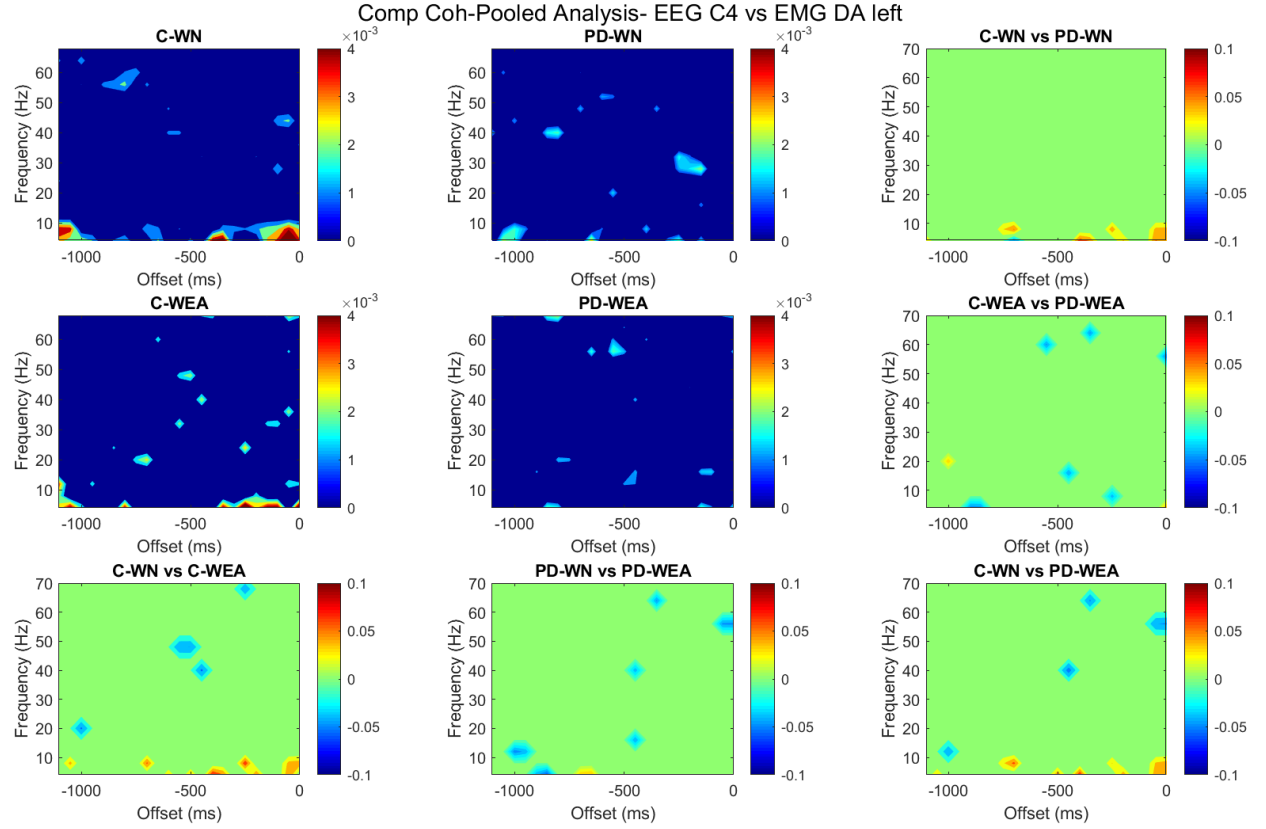


Figure 31: Shows  $T_d$  comparison of coherences for the four groups for cortical region C4 and muscle DA of the left shoulder.

## 4. Discussion

The analyses of EEG and EMG signal were done to find out synergies in cortical activity and motor action. Tasks like walking and simple cues like normal and enhanced arm swing (both are anti phase) with that were used to find out its effect on stimulus in cortical region, and motor action of leg and arm muscles. Three questions were posed in the Introduction section, using the methodology of time-frequency analyses to calculate and compare estimates of coherence, phase and cumulant density has tried to answer the questions posed.

Firstly, it was asked if M1 is involved in leg muscle activation during gait. This question can be answered with the basic concepts of coherence and cumulant density. In frequency or time domain, analysis of the estimates of coherence or cumulant density, respectively, if are significant, indicate correlation between signals, as described in Halliday et al., (1995). The EEG signals from cortical region Cz and EMG signals from leg muscles TA and RF have shown a bi-directional corticomuscular coupling in both  $T_{ind}$  and  $T_d$  analyses, which strongly indicates information interaction between M1 and leg muscles TA and RF, confirming M1 is involved in leg muscle activation during gait. If M1 was not involved in leg muscle activation, the correlation would have been insignificant as it was shown in demos in the user guide of NeuroSpec Version 2.0, where two random datasets were generated and analysed for Type 1 analysis (<http://www.neurospec.org/>).

Furthermore, in the second question it was asked if SMA, directly or indirectly through M1 is involved in the activation of leg muscles during gait. The involvement of SMA can be found by looking into the correlations between EEG signals from cortical region Fz and EMG signals from leg muscles TA and RF. Significant estimates of coherence and cumulant density and a bi-directional corticomuscular coupling in both  $T_{ind}$  and  $T_d$  analyses indicate that SMA is involved in leg muscle activation. Yang et. al., (2006) says, although walking seems relatively effortless, motor commands are required for the stability. Also, study in Holtzer et al., (2011) and Koenraadt et al., (2014) have documented SMA's activation in walking and running gaits. These studies indicate that SMA can be directly involved in planning and stability. Thus, the activation in SMA indirectly through M1 can be involved in leg muscle activation during gait.

Subsequently, the third question asks if SMA and M1 are involved in activation of arm muscles during gait related arm swing. This can be answered by comparing a case of walking normal to walking with enhanced arm swing. Four cases in section Comparison of Coherence

i.e. Cz vs TA, Fz vs TA, Cz vs RF, and Fz vs RF (figures 26, 27, 28 and 29, respectively) demonstrate the estimate of coherence changes when walked with enhanced arm swing. This indicates that SMA and M1 both are involved in activation of arm muscles during gait related arm swing.

Additionally, in section Comparison of Coherence, while comparing Cz vs TA coherence, it was observed that excess coherence of PD\_WN in PD\_WN vs PD\_WEA during midstand, go away in C\_WN vs PD\_WEA. Also, when compared Fz with TA, it was noticed that excess beta and gamma frequency coherence, in C\_WN vs PD\_WN vanishes away in C\_WN vs PD\_WEA comparison. These outcomes indicate that walking with enhanced arm has helped to bring PD\_WEA much closer to C\_WN.

In all the cases, there is corticomuscular correlation present in multiple frequency bands and during enhanced arm movements the correlation can be seen changing over these bands, which indicates a possibility of different mechanisms involved. although corticomuscular correlation already have been demonstrated to be highly nonlinear (Darvas et al., 2009; Chen et al., 2010; Yang et al., 2016c), most of the studies have only used the linear part of this corticomuscular correlation to understand the neuronal communication. The technique used in NeuroSpec and (Halliday et al., 1995) is also based on linear pairwise interactions. An alternative non-linear analysis technique where higher order spectra of order greater than 2, defined as higher order cumulants will address the problem in a better way because they hold much more information than auto spectra and cross spectra (Petropulu, 1994).

Understanding phase and cumulant density estimates where coherence is significant would have helped to understand the directionality which is not done under this assignment. Also, if the data were normalized between the heel strikes would have given the true representation of the pooled analysis and comparison of coherences.

## **5. Conclusion**

In the present work corticomuscular correlations were studies employing EEG signals from cortical and surface EMG from leg and arm muscles. Enhanced arm swings while walking were used as a cue to investigate the activation in M1 and SMA to find out its effect in PD patients. Multiple scripts in MATLAB R2018a were written to interconnect the functions defined in NeuroSpec (<http://www.neurospec.org/>) to find out the estimate of significant correlations in time and frequency domain. Comparing control and PD groups for estimate of coherence has suggested that enhanced arm swings while walking try to bridge the gap of corticomuscular correlations amid control and Parkinson's disease patients.

## **6. Acknowledgment**

I am grateful to David M. Halliday and his peers for programming the analysis software that was used for the calculations. I also am thankful to the participants who have contributed in building the dataset. This work required initial training to understand the scripts written in the analysis software. Prof. Natasha M. Maurits and Ms. Joyce B. Weersink helped me in understanding the scripts and their outcomes. I am thankful to them for providing me the opportunity to work with them and helping me throughout the whole internship.

## 7. References

1. Amjad, A., Halliday, D., Rosenberg, J. & Conway, B. (1997), An extended difference of coherence test for comparing and combining several independent coherence estimates: theory and application to the study of motor units and physiological tremor. *Journal of Neuroscience Methods*, 73, 69-79.
2. Annett M. (1970), A classification of hand preference by association analysis. *Br. J. Psychol.* 61 303–321.
3. Artoni, F., Fanciullacci, C., Bertolucci, F., Panarese, A., Makeig, S., Micera, S. & Chisari, C. (2017), Unidirectional brain to muscle connectivity reveals motor cortex control of leg muscles during stereotyped walking. *NeuroImage*, 159, 403-416.
4. Bloomfield Fourier, P. (1976), *Analysis of Time Series: An Introduction*. 1st Editon, John Wiley and Sons, Hoboken.
5. Brillinger, D. R. (1993), The digital rainbow: Some history and applications of numerical spectrum analysis. *Can J Statistics*, 21: 1-19. doi:10.2307/3315653.
6. Brillinger, D. R. (1974), Fourier analysis of stationary processes. *Proc. IEEE*, 62: 1628–1643.
7. Chen C.-C., Kilner J. M., Friston K. J., Kiebel S. J., Jolly R. K., Ward N. S. (2010), Nonlinear coupling in the human motor system. *J. Neurosci.* 30, 8393–8399. 10.1523/JNEUROSCI.1194-09.2010.
8. Darvas, F., Ojemann, J.G., Sorensen, L.B. (2009), Bi-phase locking — a tool for probing non-linear interaction in the human brain, *NeuroImage*, Volume 46, Issue 1, Pages 123-132, ISSN 1053-8119.
9. Dyer J.O., Maupas E., Melo S.A., Bourbonnais D., Nadeau S., Forget R. (2014), Changes in activation timing of knee and ankle extensors during gait are related to changes in heteronymous spinal pathways after stroke. *Journal of NeuroEngineering and Rehabilitation*, 11:148, <https://doi.org/10.1186/1743-0003-11-148>.
10. Gazzaniga M., Ivry R., & Mangun G., (2002), *Cognitive neuroscience: The biology of the mind*, second edn, New York: Norton.
11. Halliday, D., Conway, B., Christensen, Hansen, N., Petersen, N. & Nielsen (2003), Functional coupling of motor units is modulated during walking in human subjects. *J Neurophysiol*, 89, 960-968.
12. Halliday, D., & Farmer, S., (2010), On the need for rectification of surface EMG. *J Neurophysiology* 103, 3547.

13. Halliday, D., Rosenberg, J., Amjad, A., Breeze, P., Conway, B. & Farmer, S. (1995), A framework for the analysis of mixed time series/point process data-theory and application to the study of physiological tremor, single motor unit discharges and electromyograms. *Prog Biophys Mol Biol* 64, 237-278.
14. Holtzer R., Mahoney J. R., Izzetoglu M., Izzetoglu K., Onaral B., Verghese J. (2011), fNIRS study of walking and walking while talking in young and old individuals. *J. Gerontol. A Biol. Sci. Med. Sci.* 66, 879–887 10.1093/gerona/glr068.
15. Jackson K.M., Joseph J., Wyard S.J., (1978), A mathematical model of arm swing during human locomotion. *Journal of Biomechanics*, Volume 11, Issues 6–7, 1978, Pages 277-289, ISSN 0021-9290, [https://doi.org/10.1016/0021-9290\(78\)90061-1](https://doi.org/10.1016/0021-9290(78)90061-1).
16. Jensen, P., Frisk, R., Spedden, M.E., Geertsen, S.S., Bouyer, L.J., Halliday, D.M., Nielsen, J.B., (2019), Using Corticomuscular and Intermuscular Coherence to Assess Cortical Contribution to Ankle Plantar Flexor Activity During Gait. *Journal of Motor Behavior*, DOI: 10.1080/00222895.2018.1563762.
17. Kiehn, O. (2016), Decoding the organization of spinal circuits that control locomotion. *Nature Reviews Neuroscience*, 17 (4), 224–238. doi:10.1038/nrn.2016.9.
18. Kuhtz-Buschbeck J.P., Jing B. (2012), Activity of upper limb muscles during human walking. *Journal of Electromyography and Kinesiology*, Volume 22, Issue 2, Pages 199-206, ISSN 1050-6411, <https://doi.org/10.1016/j.jelekin.2011.08.014>.
19. Koenraadt K. L., Duysens J., Smeenk M., Keijsers N. L. (2012), Multi-channel NIRS of the primary motor cortex to discriminate hand from foot activity. *J. Neural Eng.* 9:046010 10.1088/1741-2560/9/4/046010.
20. Petersen, T. H., Willerslev-Olsen, M., Conway, B. & Nielsen, J. (2012), The motor cortex drives the muscles during walking in human subjects. *The Journal of Physiology*, 590(Pt 10), 2443-2452.
21. Petropulu A.P. (1994), Higher-Order Spectra in Biomedical Signal Processing, IFAC Proceedings Volumes, Volume 27, Issue 1, Pages 47-52, ISSN 1474-6670, [https://doi.org/10.1016/S1474-6670\(17\)46158-1](https://doi.org/10.1016/S1474-6670(17)46158-1).
22. Rosenberg, J.R., Amjad, A.M., Breeze, P., Brillinger, D.R. and Halliday, D.M. (1989), The Fourier approach to the identification of functional coupling between neuronal spike trains. *Prog. Biophys. Mol. Biol.*, 53: 1–31.
23. Rouiller E.M., Babalian A., Kazennikov O., Moret V., Yu X.H., Wiesndanger M. (1994), Transcallosal connections of the distal forelimb representations of the primary and supplementary motor cortical areas in macaque monkeys. *Exp. Brain Res.* 102 227–243.

24. Ruddy K.L., Leemans A., Carson R.G. (2017), Transcallosal connectivity of the human cortical motor network. *Brain Struct. Funct.* 222 1243–1252.
25. Sejdic E., Lowry K.A., Bellanca J., Perera S., Redfern M.S., Brach J.S. (2016), Extraction of stride events from gait accelerometry during treadmill walking. *IEEE J. Transl. Eng. Heal. Med.* 4, 1–11.
26. Shapiro, L. J., & Jungers, W. L. (1994), Electromyography of back muscles during quadrupedal and bipedal walking in primates. *American Journal of Physical Anthropology*, 93 (4), 491–504. doi:10.1002/ajpa.1330930408
27. Suwansawang, S., (2018), Analysis of human locomotion using analytic wavelets applied to electromyographic data from healthy controls and Parkinson's patients. PhD thesis, University of York.
28. Trank, T. V., Chen, C., & Smith, J. L. (1996), Forms of forward quadrupedal locomotion. I. A comparison of posture, hindlimb kinematics, and motor patterns for normal and crouched walking. *Journal of Neurophysiology*, 76 (4), 2316–2326.
29. Vaughan, C., Davis, B. & O'Connor, J. (1999), Dynamics of human gait, second edn, Kiboho Publishers, Cape Town, South Africa.
30. Weersink, J.B., Maurits, N.M., Jong, B. M. (2019), EEG time-frequency analysis provides arguments for arm swing support in human gait control. *Gait & Posture*, Volume 70, Pages 71-78, ISSN 0966-6362, <https://doi.org/10.1016/j.gaitpost.2019.02.017>.
31. Yang J. F., Gorassini M. (2006), Spinal and brain control of human walking: implications for retraining of walking. *Neuroscientist* 12, 379–389 10.1177/1073858406292151.
32. Yang Y., Solis-Escalante T., Yao J., van der Helm F. C. T., Dewald J. P. A., Schouten A. C. (2016c), Nonlinear connectivity in the human stretch reflex assessed by cross-frequency phase coupling. *Int. J. Neural Syst.* 26:1650043. 10.1142/s012906571650043.

## 8. Appendix

### 8.1 Participant data

Table 2: Participant characteristic data

<b>Identification Number</b>	<b>Group</b>	<b>Age</b>	<b>Gender</b>	<b>MMSE</b>	<b>Levodopa equivalent dosage</b>
31	C	56	f	29	
32	C	67	m	30	
33	PD	73	m	29	400
34	C	70	f	30	
35	C	69	m	30	
36	C	71	f	26	
37	C	67	f	28	
38	PD	68	m	27	500
39	C	71	f	29	
40	PD	54	f	30	995
41	PD	69	f	30	750
42	C	75	m	29	
43	PD	70	m	28	800
44	C	69	f	28	
45	C	70	m	30	
46	C	61	m	29	
47	PD	68	m	25	450
48	PD	61	m	30	1180
49	C	71	m	30	
50	PD	71	m	29	1098
51	PD	74	m	25	1100
52	PD	57	f	28	1000
53	PD	73	m	29	1848
54	C	68	m	30	
55	C	56	m	29	
56	PD	65	f	27	1380
57	C	74	f	28	
58	C	73	f	30	
59	C	70	m	27	
60	PD	52	f	30	599
61	C	69	f	29	
62	C	48	m	29	
63	C	66	f	30	
64	PD	61	f	28	363
65	PD	60	f	30	988
66	PD	77	m	28	538
67	PD	71	m	30	540
68	PD	59	m	28	300
69	PD	67	m	29	500
70	PD	59	m	24	1300

## 8.2 Time Independent Analysis

### 8.2.1 EEG data from cortical region Cz vs EMG data from TA

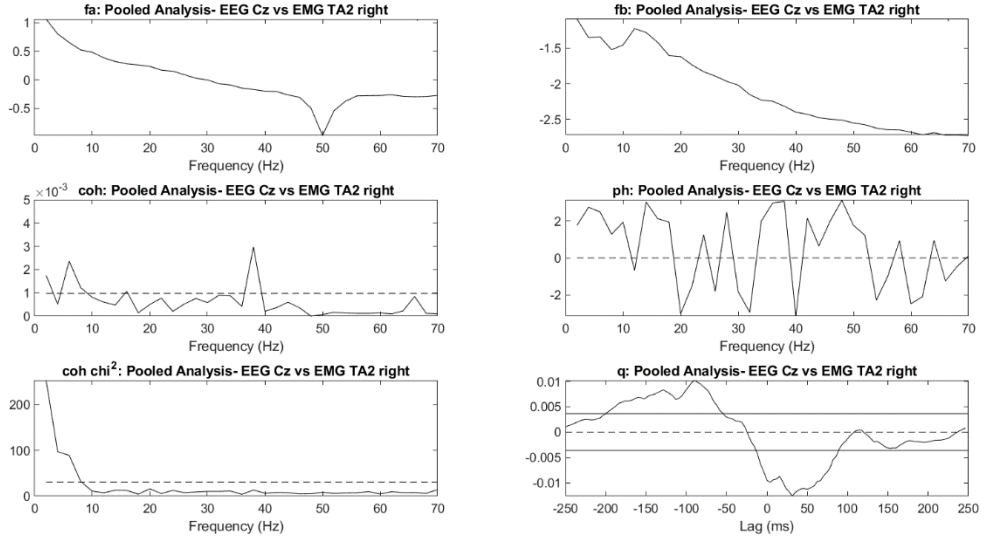


Figure 32: Shows pooled estimates of corticomuscular coupling parameters for C\_WN, i.e. EEG spectra (top-left), EMG spectra (top-right), coherence (middle-left), phase (middle-right), chi-square coherence (bottom-left), cumulant density (bottom-right) for cortical region Cz and muscle TA of right leg and between offset -550 ms to 0 ms.

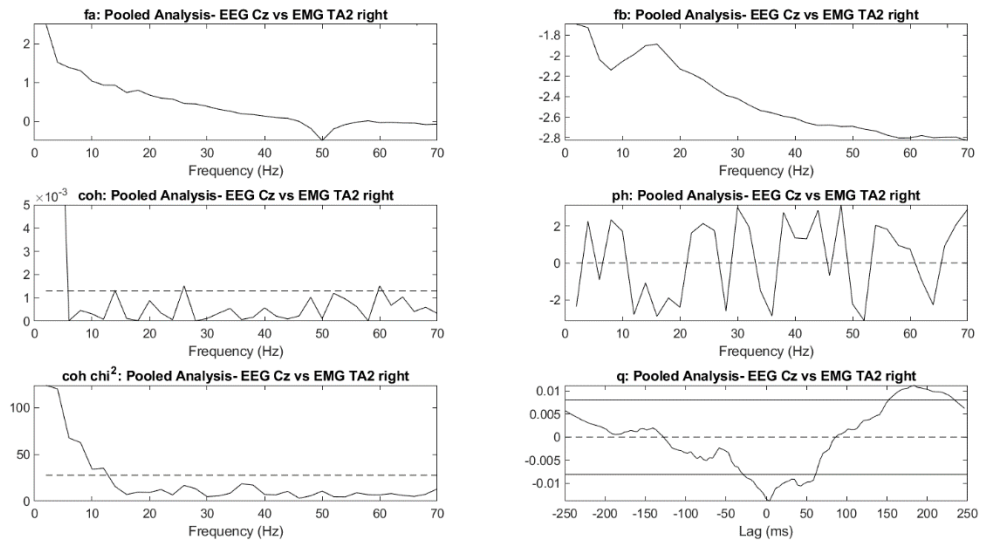


Figure 33: Shows pooled estimates of corticomuscular coupling parameters for C\_WEA, i.e. EEG spectra (top-left), EMG spectra (top-right), coherence (middle-left), phase (middle-right), chi-square coherence (bottom-left), cumulant density (bottom-

right) for cortical region Cz and muscle TA of right leg and between offset -550 ms to 0 ms.

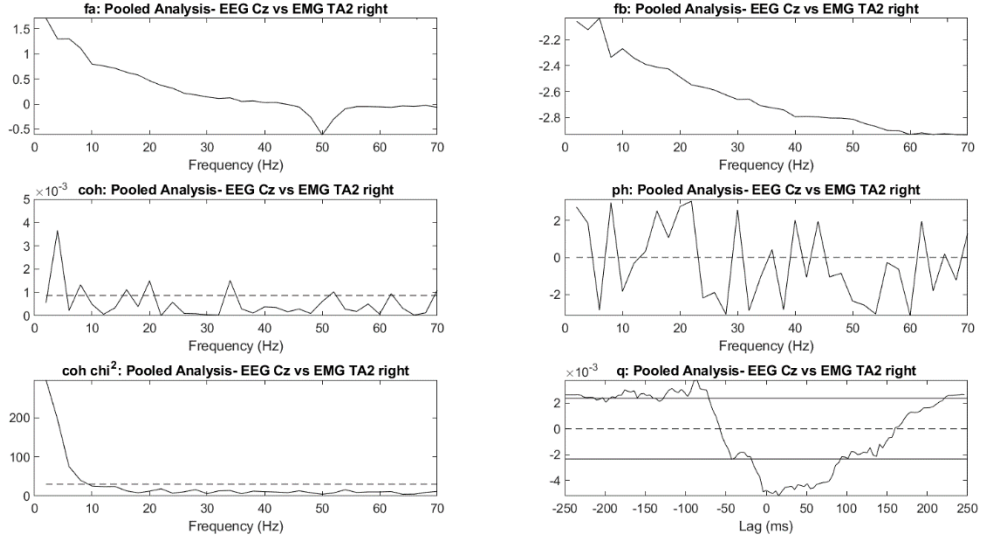


Figure 34: Shows pooled estimates of corticomuscular coupling parameters for PD\_WN, i.e. EEG spectra (top-left), EMG spectra (top-right), coherence (middle-left), phase (middle-right), chi-square coherence (bottom-left), cumulant density (bottom-right) for cortical region Cz and muscle TA of right leg and between offset -550 ms to 0 ms.

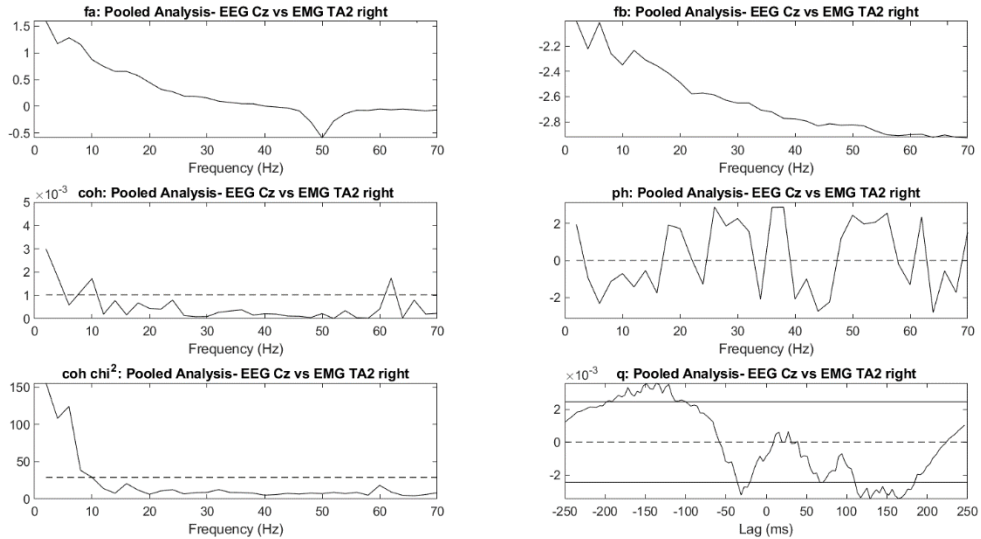


Figure 35: Shows pooled estimates of corticomuscular coupling parameters for PD\_WEA, i.e. EEG spectra (top-left), EMG spectra (top-right), coherence (middle-left), phase (middle-right), chi-square coherence (bottom-left), cumulant density (bottom-right) for cortical region Cz and muscle TA of right leg and between offset -550 ms to 0 ms.

right) for cortical region Cz and muscle TA of right leg and between offset -550 ms to 0 ms.

### 8.2.2 EEG data from cortical region Fz vs EMG data from TA

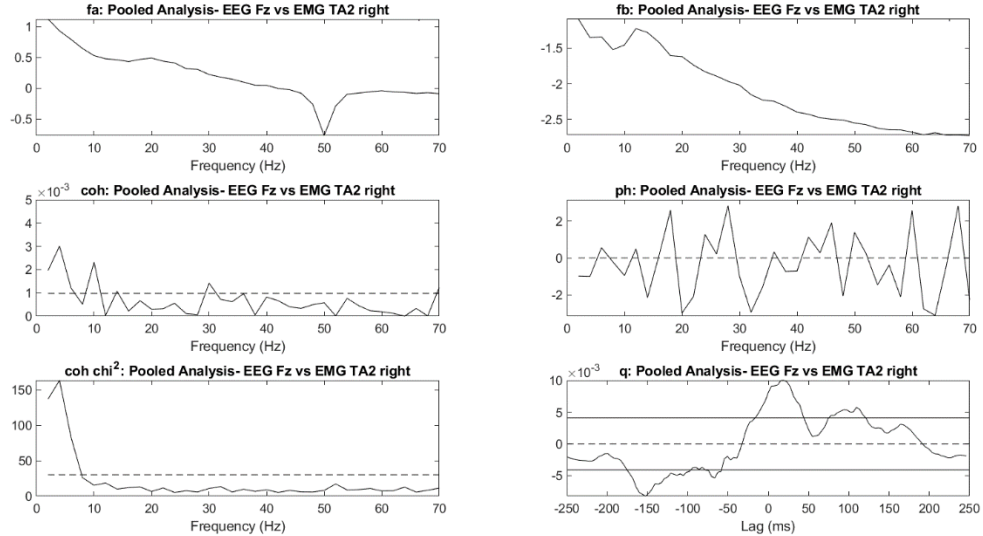


Figure 36: Shows pooled estimates of corticomuscular coupling parameters for C\_WN, i.e. EEG spectra (top-left), EMG spectra (top-right), coherence (middle-left), phase (middle-right), chi-square coherence (bottom-left), cumulant density (bottom-right) for cortical region Fz and muscle TA of right leg and between offset -550 ms to 0 ms.

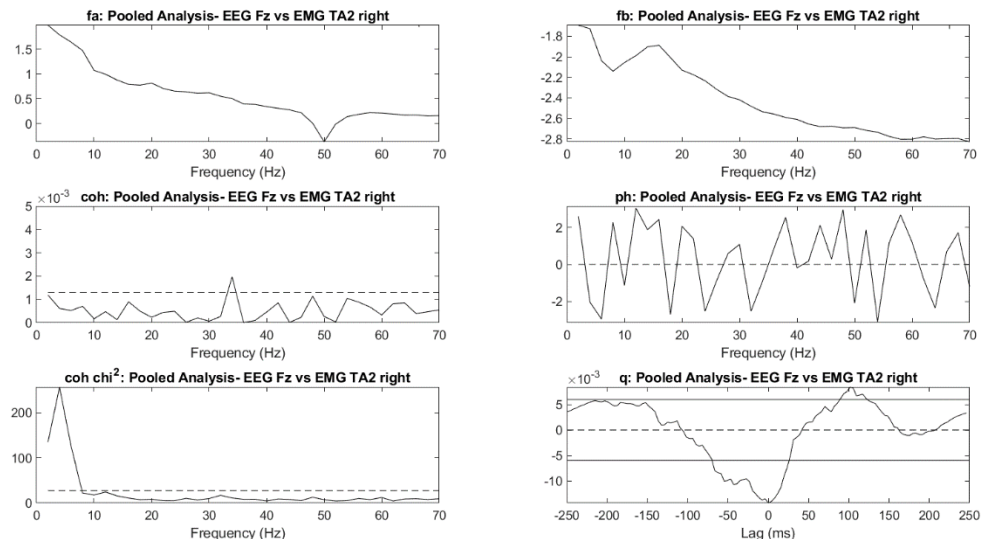


Figure 37: Shows pooled estimates of corticomuscular coupling parameters for C\_WEA, i.e. EEG spectra (top-left), EMG spectra (top-right), coherence (middle-left),

phase (middle-right), chi-square coherence (bottom-left), cumulant density (bottom-right) for cortical region Fz and muscle TA of right leg and between offset -550 ms to 0 ms.

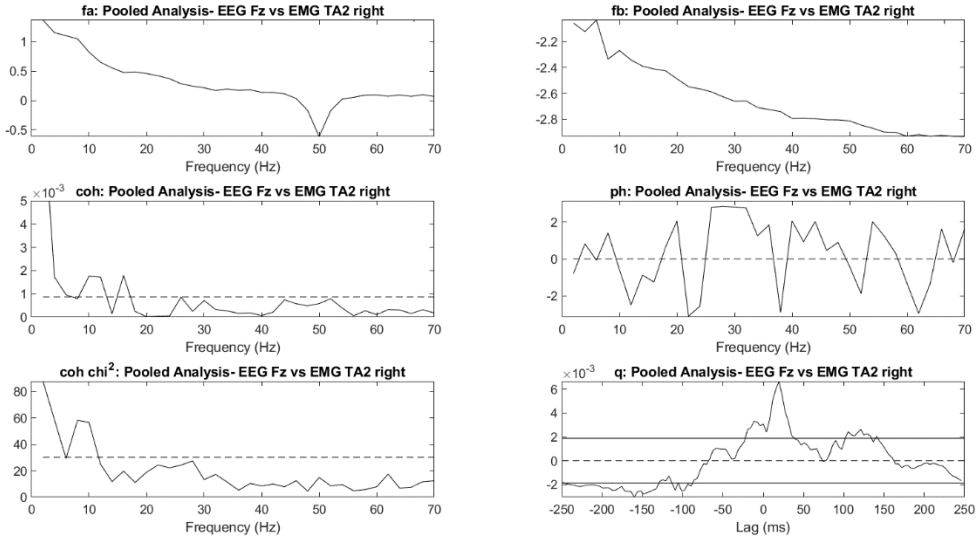


Figure 38: Shows pooled estimates of corticomuscular coupling parameters for PD\_WN, i.e. EEG spectra (top-left), EMG spectra (top-right), coherence (middle-left), phase (middle-right), chi-square coherence (bottom-left), cumulant density (bottom-right) for cortical region Fz and muscle TA of right leg and between offset -550 ms to 0 ms.

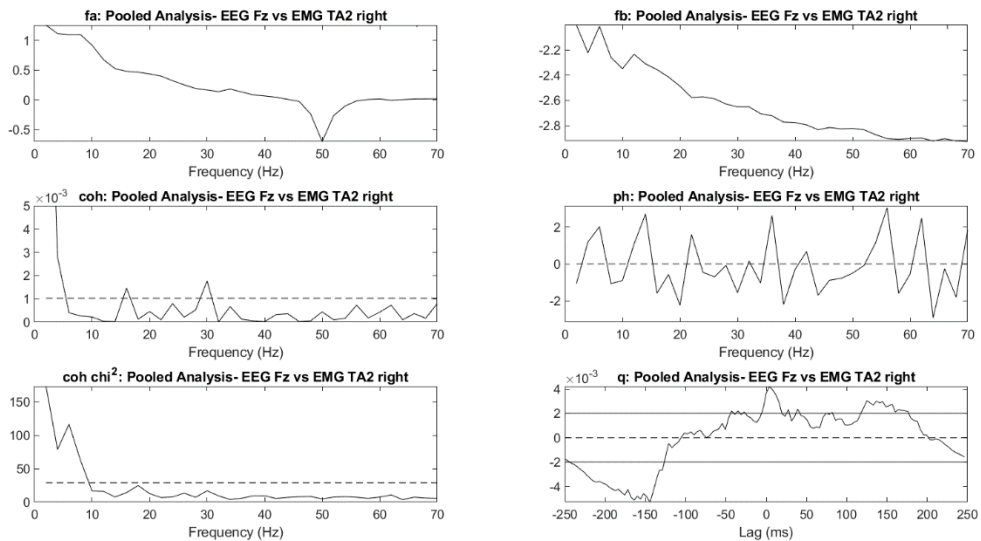


Figure 39: Shows pooled estimates of corticomuscular coupling parameters for PD\_WEA, i.e. EEG spectra (top-left), EMG spectra (top-right), coherence (middle-left),

phase (middle-right), chi-square coherence (bottom-left), cumulant density (bottom-right) for cortical region Fz and muscle TA of right leg and between offset -550 ms to 0 ms.

### 8.2.3 EEG data from cortical region Cz vs EMG data from RF

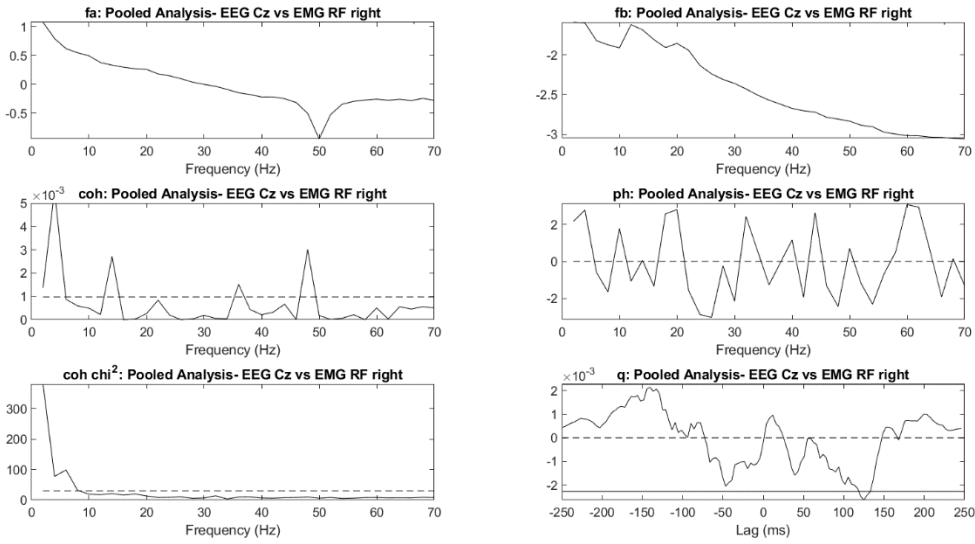


Figure 40: Shows estimates of corticomuscular coupling parameters for C\_WN, i.e. EEG spectra (top-left), EMG spectra (top-right), coherence (middle-left), phase (middle-right), chi-square coherence (bottom-left), cumulant density (bottom-right) for cortical region Cz and muscle RF of right leg and between offset -1100 ms to -600 ms.

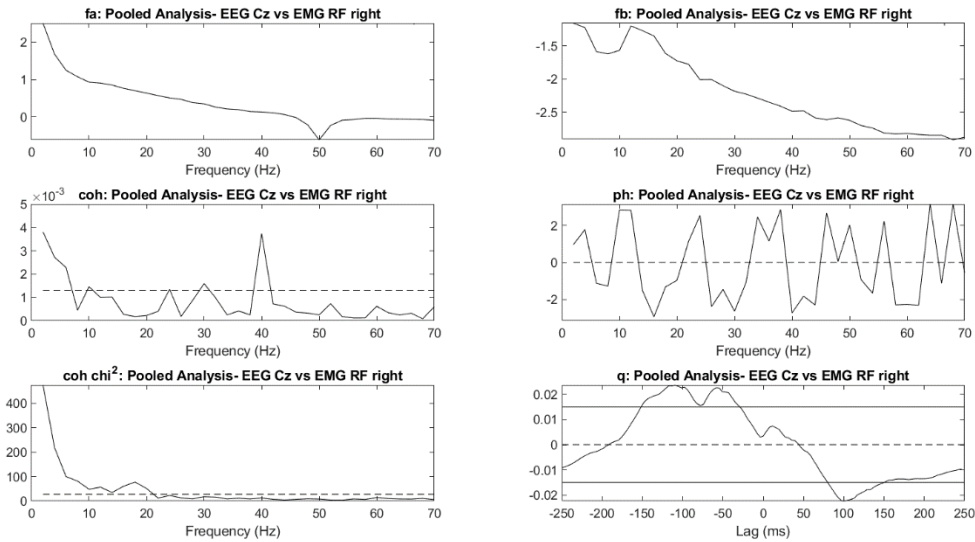


Figure 41: Shows pooled estimates of corticomuscular coupling parameters for C\_WEA, i.e. EEG spectra (top-left), EMG spectra (top-right), coherence (middle-left), phase (middle-right), chi-square coherence (bottom-left), cumulant density (bottom-right) for cortical region Cz and muscle RF of right leg and between offset -1100 ms to -600 ms.

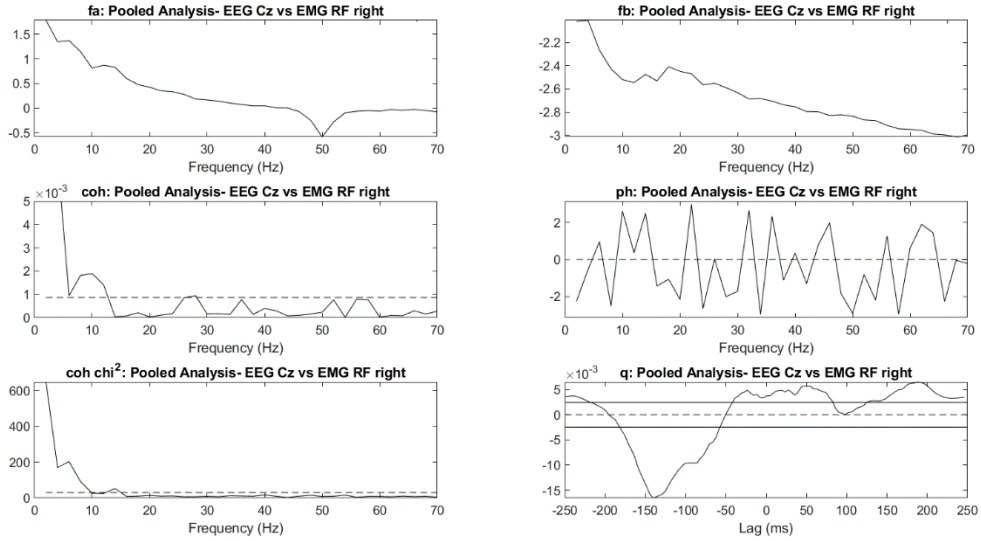


Figure 42: Shows pooled estimates of corticomuscular coupling parameters for PD\_WN, i.e. EEG spectra (top-left), EMG spectra (top-right), coherence (middle-left), phase (middle-right), chi-square coherence (bottom-left), cumulant density (bottom-right) for cortical region Cz and muscle RF of right leg and between offset -1100 ms to -600 ms.

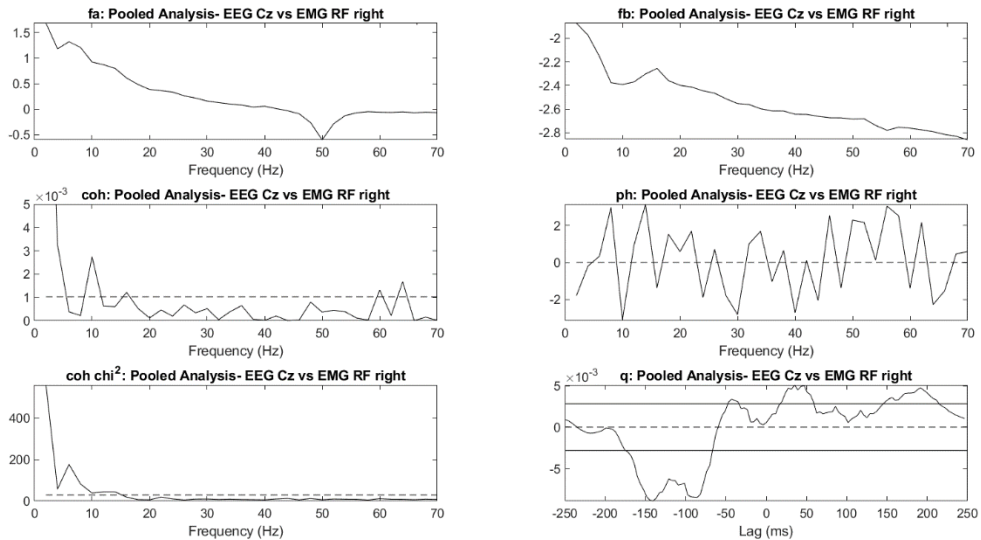


Figure 43: Shows pooled estimates of corticomuscular coupling parameters for PD\_WEA, i.e. EEG spectra (top-left), EMG spectra (top-right), coherence (middle-left), phase (middle-right), chi-square coherence (bottom-left), cumulant density (bottom-right) for cortical region Cz and muscle RF of right leg and between offset -1100 ms to -600 ms.

#### 8.2.4 EEG data from cortical region Fz vs EMG data from RF

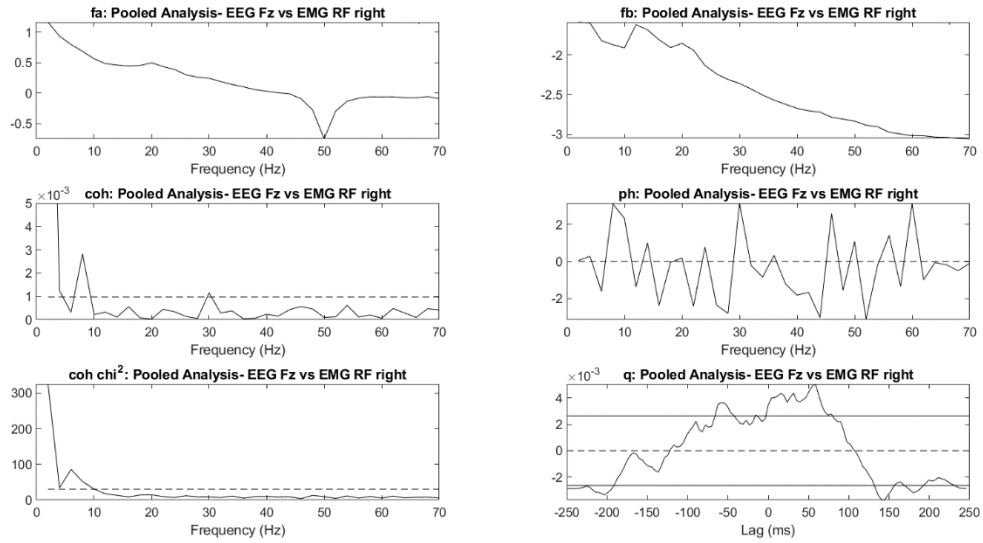


Figure 44: Shows pooled estimates of corticomuscular coupling parameters for C\_WN, i.e. EEG spectra (top-left), EMG spectra (top-right), coherence (middle-left), phase (middle-right), chi-square coherence (bottom-left), cumulant density (bottom-right) for cortical region Fz and muscle RF of right leg and between offset -1100 ms to -600 ms.

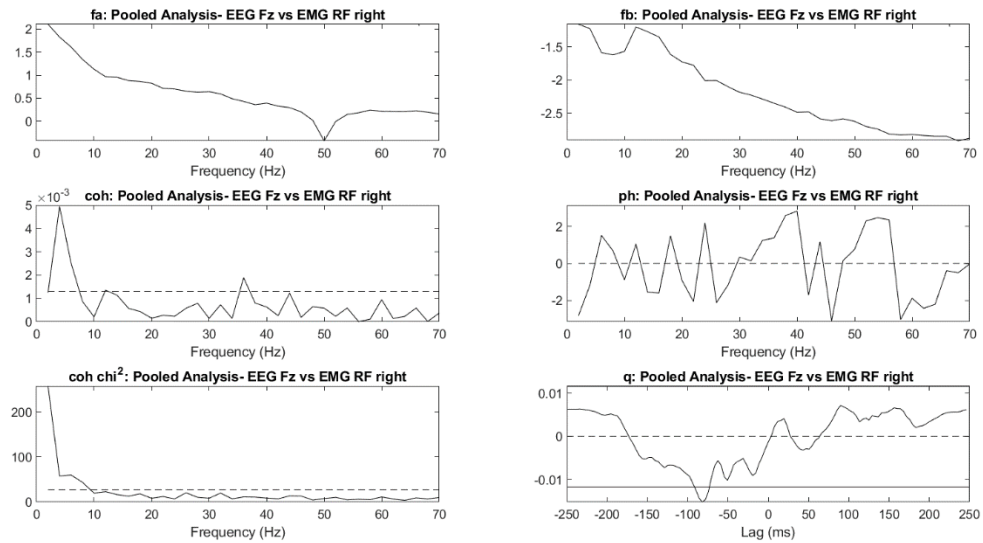


Figure 45: Shows pooled estimates of corticomuscular coupling parameters for C\_WEA, i.e. EEG spectra (top-left), EMG spectra (top-right), coherence (middle-left), phase (middle-right), chi-square coherence (bottom-left), cumulant density (bottom-right) for cortical region Fz and muscle RF of right leg and between offset -1100 ms to -600 ms.

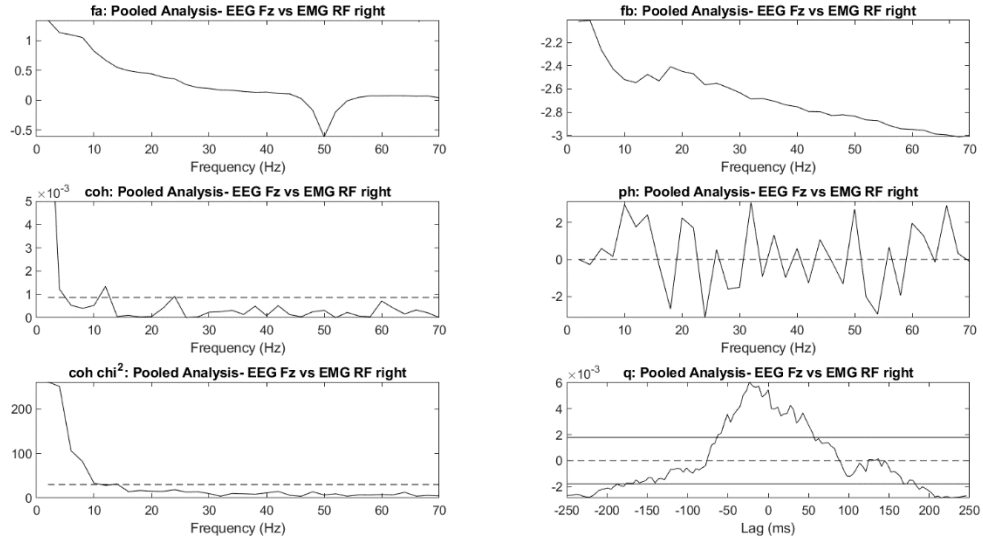


Figure 46: Shows pooled estimates of corticomuscular coupling parameters for PD\_WN, i.e. EEG spectra (top-left), EMG spectra (top-right), coherence (middle-left), phase (middle-right), chi-square coherence (bottom-left), cumulant density (bottom-right) for cortical region Fz and muscle RF of right leg and between offset -1100 ms to -600 ms.

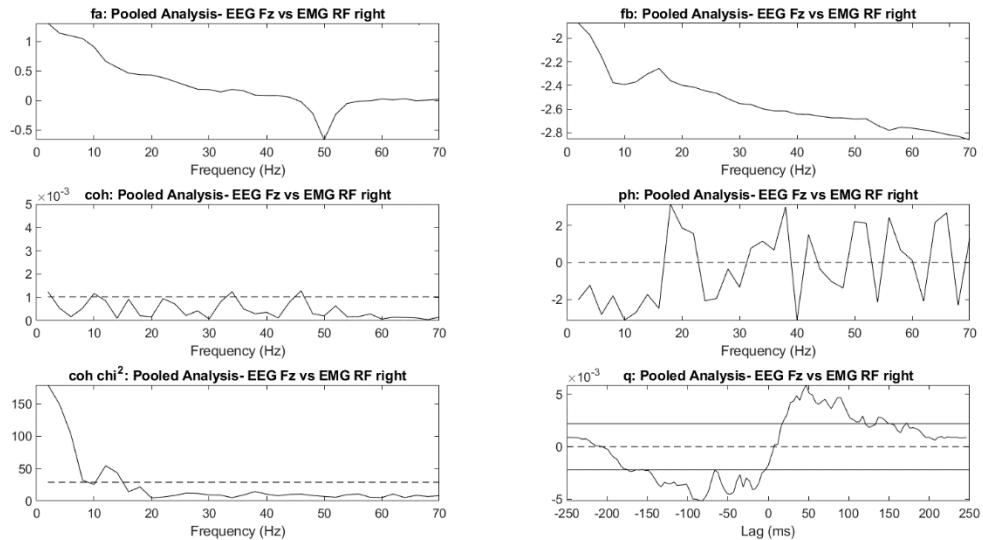


Figure 47: Shows pooled estimates of corticomuscular coupling parameters for PD\_WEA, i.e. EEG spectra (top-left), EMG spectra (top-right), coherence (middle-left), phase (middle-right), chi-square coherence (bottom-left), cumulant density (bottom-right) for cortical region Fz and muscle RF of right leg and between offset -1100 ms to -600 ms.

### 8.2.5 EEG data from cortical region Fz vs EMG data from DA (left)

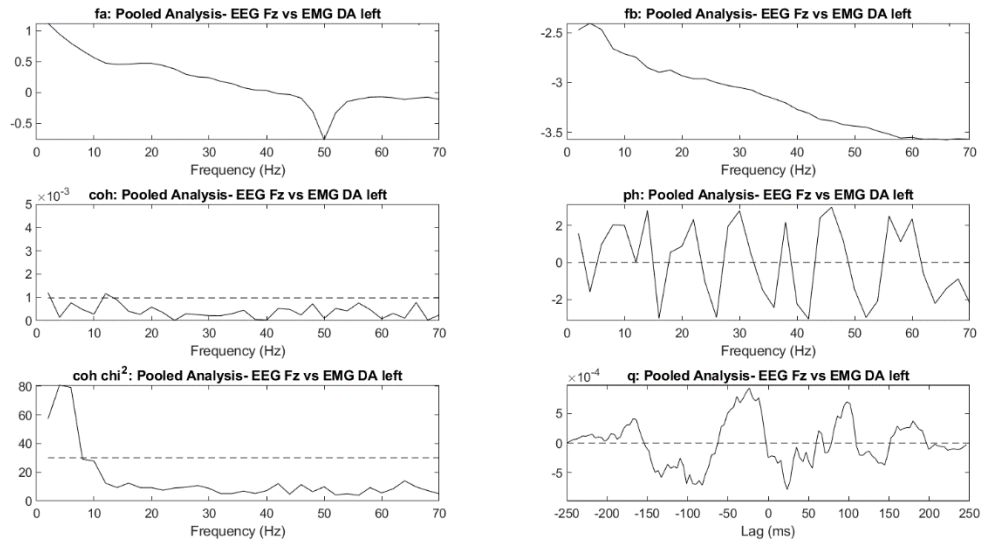


Figure 48: Shows pooled estimates of corticomuscular coupling parameters for C\_WN, i.e. EEG spectra (top-left), EMG spectra (top-right), coherence (middle-left), phase (middle-right), chi-square coherence (bottom-left), cumulant density (bottom-right) for cortical region Fz and muscle DA of left arm and between offset -950 ms to -450 ms.

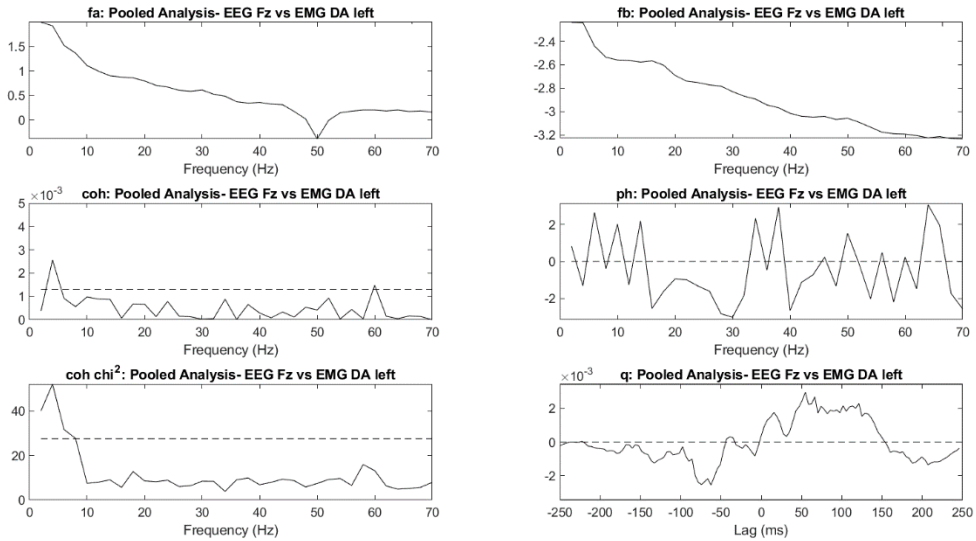


Figure 49: Shows pooled estimates of corticomuscular coupling parameters for C\_WEA, i.e. EEG spectra (top-left), EMG spectra (top-right), coherence (middle-left), phase (middle-right), chi-square coherence (bottom-left), cumulant density (bottom-right) for cortical region Fz and muscle DA of left arm and between offset -950 ms to -450 ms.

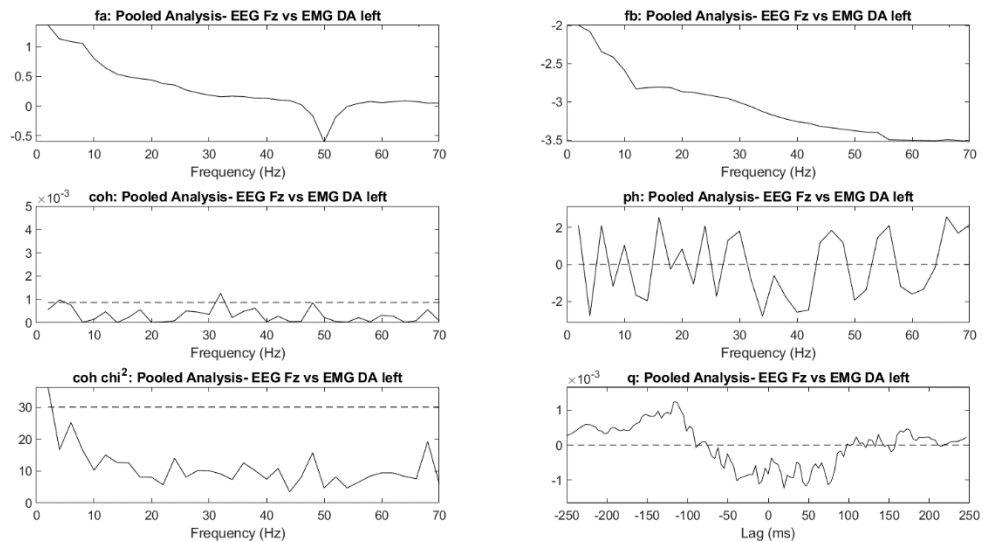


Figure 50: Shows pooled estimates of corticomuscular coupling parameters for PD\_WN, i.e. EEG spectra (top-left), EMG spectra (top-right), coherence (middle-left), phase (middle-right), chi-square coherence (bottom-left), cumulant density (bottom-right) for cortical region Fz and muscle DA of left arm and between offset -950 ms to -450 ms.

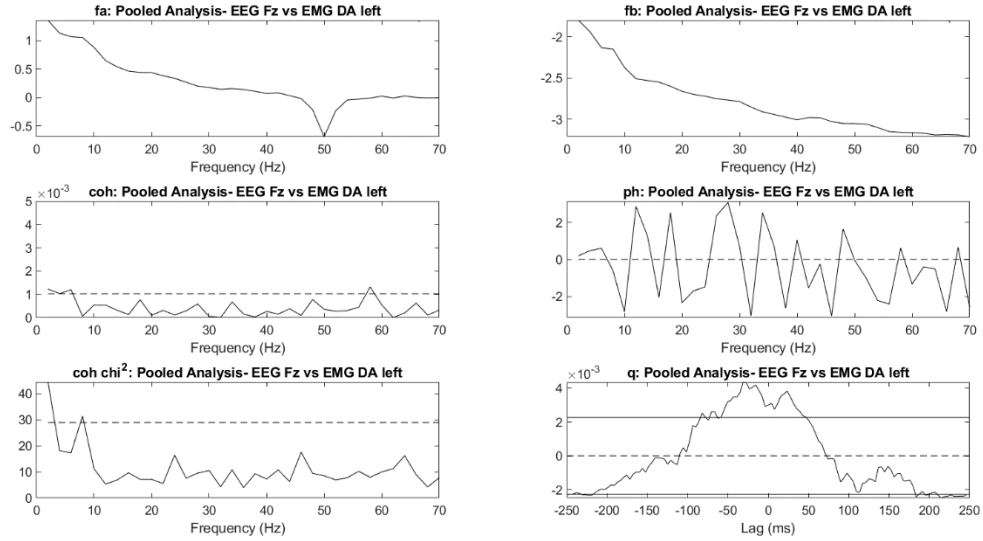


Figure 51: Shows pooled estimates of corticomuscular coupling parameters for PD\_WEA, i.e. EEG spectra (top-left), EMG spectra (top-right), coherence (middle-left), phase (middle-right), chi-square coherence (bottom-left), cumulant density (bottom-right) for cortical region Fz and muscle DA of left arm and between offset -950 ms to -450 ms.

### 8.2.6 EEG data from cortical region C4 vs EMG data from DA (left)

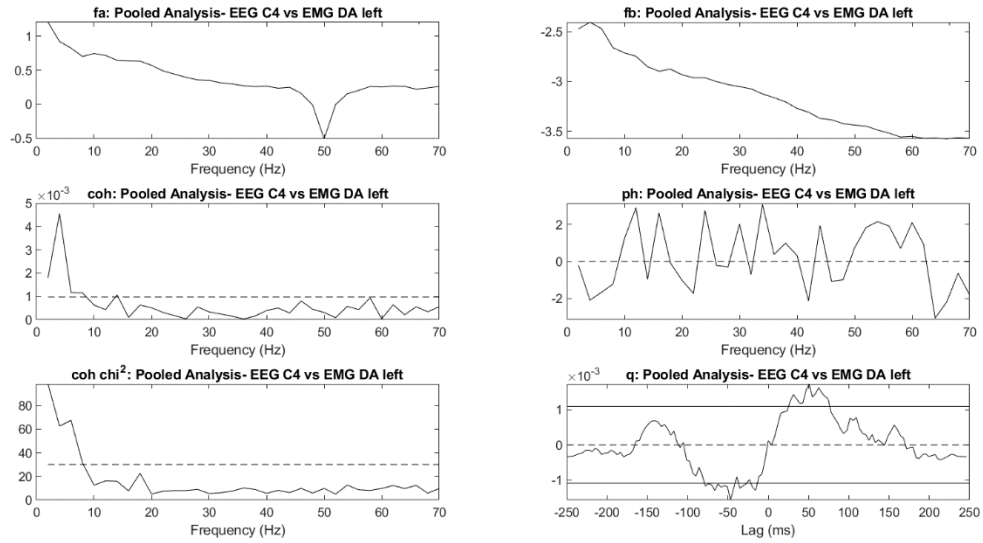


Figure 52: Shows pooled estimates of corticomuscular coupling parameters for C\_WN, i.e. EEG spectra (top-left), EMG spectra (top-right), coherence (middle-left), phase (middle-right), chi-square coherence (bottom-left), cumulant density (bottom-right) for cortical region C4 and muscle DA of left arm and between offset -950 ms to -450 ms.

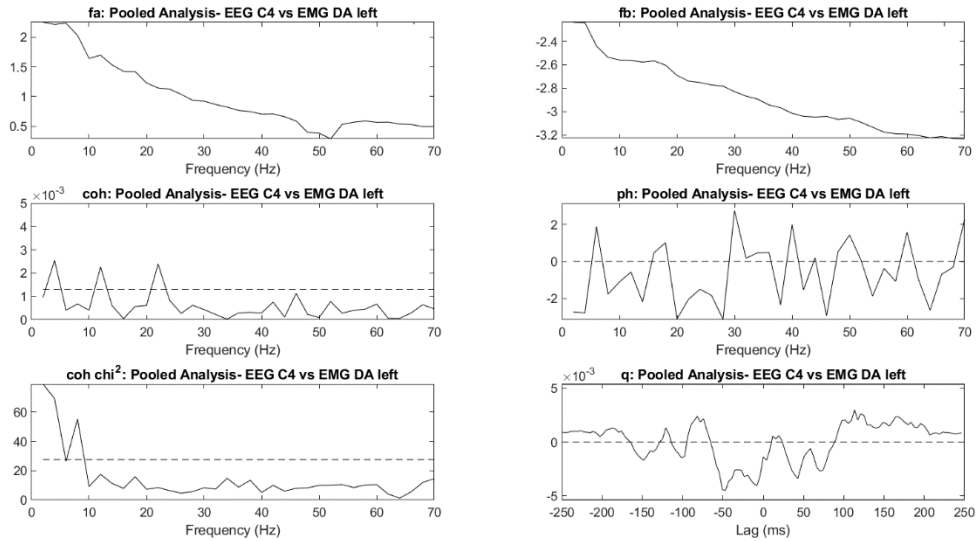


Figure 53: Shows pooled estimates of corticomuscular coupling parameters for C\_WEA, i.e. EEG spectra (top-left), EMG spectra (top-right), coherence (middle-left), phase (middle-right), chi-square coherence (bottom-left), cumulant density (bottom-right) for cortical region C4 and muscle DA of left arm and between offset -950 ms to -450 ms.

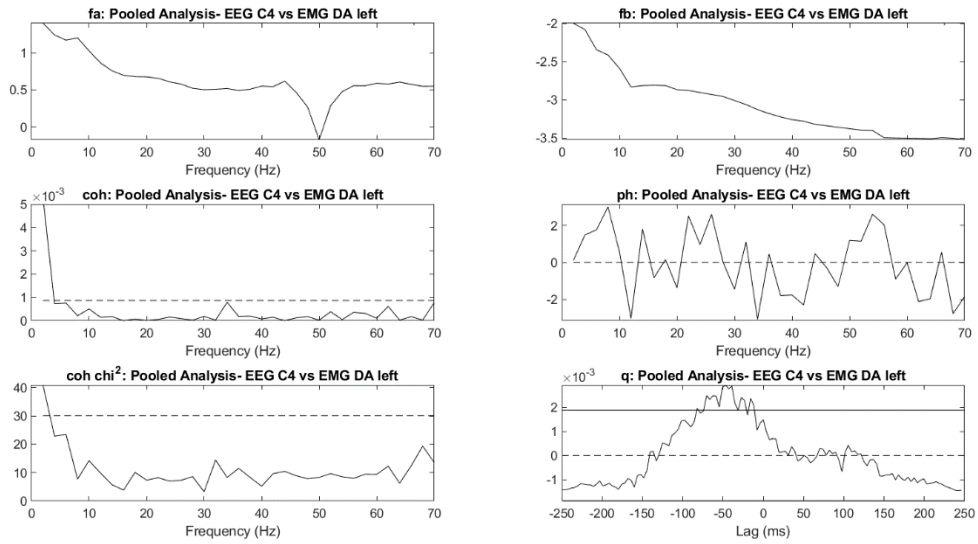


Figure 54: Shows pooled estimates of corticomuscular coupling parameters for PD\_WN, i.e. EEG spectra (top-left), EMG spectra (top-right), coherence (middle-left), phase (middle-right), chi-square coherence (bottom-left), cumulant density (bottom-right) for cortical region C4 and muscle DA of left arm and between offset -950 ms to -450 ms.

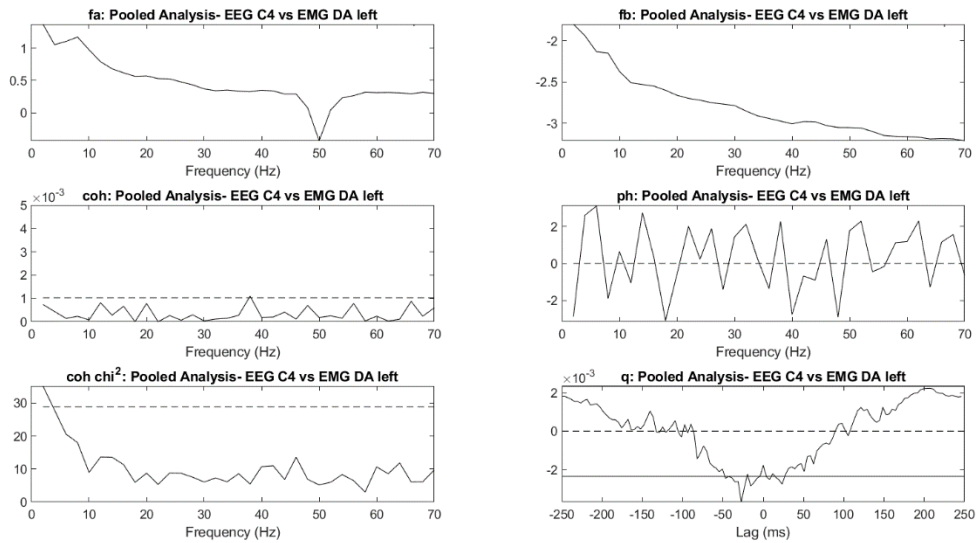


Figure 55: Shows pooled estimates of corticomuscular coupling parameters for PD\_WEA, i.e. EEG spectra (top-left), EMG spectra (top-right), coherence (middle-left), phase (middle-right), chi-square coherence (bottom-left), cumulant density (bottom-right) for cortical region C4 and muscle DA of left arm and between offset -950 ms to -450 ms.